

# Stock Options and Credit Default Swaps: A Joint Framework for Valuation and Estimation

PETER CARR

*Bloomberg LP and New York University*

LIUREN WU

*Baruch College, CUNY*

## ABSTRACT

We propose a dynamically consistent framework that allows joint valuation and estimation of stock options and credit default swaps written on the same reference company. We model default as controlled by a Cox process with a stochastic arrival rate. When default occurs, the stock price drops to zero. Prior to default, the stock price follows a jump-diffusion process with stochastic volatility. The instantaneous default rate and variance rate follow a bivariate continuous process, with its joint dynamics specified to capture the observed behavior of stock option prices and credit default swap spreads. Under this joint specification, we propose a tractable valuation methodology for stock options and credit default swaps. We estimate the joint risk dynamics using data from both markets for eight companies that span five sectors and six major credit rating classes from B to AAA. The estimation highlights the interaction between market risk (return variance) and credit risk (default arrival) in pricing stock options and credit default swaps. (*JEL*: C13, C51, G12, G13)

We thank George Tauchen (the editor), the associate editor, two anonymous referees, Gurdip Bakshi, Philip Brittan, Bjorn Flesaker, Dajiang Guo, Pat Hagan, Harry Lipman, Bo Liu, Sheikh Pancham, Louis Scott, and participants at Bloomberg, Baruch College, MIT, the 2005 Credit Risk Conference at Wharton, the 13th annual conference on Pacific Basin Finance, Economics, and Accounting at Rutgers University, the 2006 North American Winter Meeting of the Econometric Society at Boston, and the Credit Derivative Symposium at Fordham University, for comments. Liuren Wu acknowledges partial financial support from Baruch College, The City University of New York. Address correspondence to Liuren Wu, Zicklin School of Business, Baruch College, One Bernard Baruch Way, B10-225, New York, NY 10010, or e-mail: [liuren.wu@baruch.cuny.edu](mailto:liuren.wu@baruch.cuny.edu)

doi: 10.1093/jfinc/nbp010

© The Author 2009. Published by Oxford University Press. All rights reserved. For permissions, please e-mail: [journals.permissions@oxfordjournals.org](mailto:journals.permissions@oxfordjournals.org).

**KEYWORDS:** credit default swaps, default arrival rate, option pricing, return variance dynamics, stock options, time-changed Lévy processes

Markets for both stock options and credit derivatives have experienced dramatic growth in the past few years. Along with the rapid growth, it has become increasingly clear to market participants that stock option implied volatilities and credit default swap (CDS) spreads are positively linked. Furthermore, when a company defaults, the company's stock price inevitably drops by a sizeable amount. As a result, the possibility of default on a corporate bond generates negative skewness in the probability distribution of stock returns. This negative skewness is manifested in the relative pricing of stock options across different strikes. When the Black and Scholes (1973) implied volatility is plotted against some measure of moneyness at a fixed maturity, the slope of the plot is positively related to the risk-neutral skewness of the stock return distribution. Recent empirical works, for example, Cremers et al. (2008), show that CDS spreads are positively correlated with both stock option implied volatility levels and the steepness of the negative slope of the implied volatility plot against moneyness.

In this paper, we propose a dynamically consistent framework that allows joint valuation and estimation of stock options and credit default swaps written on the same reference company. We model company default as controlled by a Cox process with a stochastic arrival rate. When default occurs, the stock price drops to zero. Prior to default, we model the stock price by a jump-diffusion process with stochastic variance. The instantaneous default rate and the instantaneous variance rate follow a bivariate continuous Markov process, with its joint dynamics specified to capture the empirical evidence on stock option prices and CDS spreads.

Under this joint specification, we propose a tractable valuation methodology for stock options and CDS contracts. We estimate the joint dynamics of the default rate and the variance rate using four years of stock option prices and CDS spreads for eight reference companies that span five sectors and six major credit rating classes from B to AAA. Our estimation shows that for all eight companies, the default rate is more persistent than the variance rate under both statistical and risk-neutral measures. The statistical persistence difference manifests different degrees of predictability. The risk-neutral difference suggests that the default rate has a more long-lasting impact on the term structure of option implied volatilities and CDS spreads than does the variance rate.

The estimation also highlights the interaction between market risk (stock return variance) and credit risk (default arrival) in pricing stock options and CDS, especially for companies with significant default probabilities. Shocks to the variance rate have a relatively uniform impact on the implied volatility skew along the moneyness dimension, whereas the impacts of shocks to the default arrival rate are larger on options at low strikes than on options at high strikes. Along the option maturity dimension, the impact of variance rate shocks declines with increasing option maturity, whereas the impact of the default risk increases with

it. For companies with significant default probabilities, the contributions of the default rate and the variance rate are comparable in magnitude in certain segments of the implied volatility surface, in particular at long maturities and low strikes.

The positive empirical relation between stock option implied volatilities and CDS spreads has been recognized only recently in the academic community. As a result, efforts to capture this linkage theoretically are only in an embryonic stage. Hull, Nelken, and White (2004) link CDS spreads and stock option prices by proposing a new implementation and estimation method for the classic structural model of Merton (1974). As is well known, this early model is highly stylized as it assumes that the only source of uncertainty is a diffusion risk in the firm's asset value. As a result, stock option prices and CDS spreads have changes that are perfectly correlated locally. Thus, the empirical observation that implied volatilities and swap spreads sometimes move in opposite directions can only be accommodated by adding additional sources of uncertainty to the model. When compared to efforts based on the structural model of Merton (1974), our contribution amounts to adding consistent, interrelated, but separate dynamics to the relation between volatility and default. The CDS contracts and the stock options contain overlapping information on the market risk and the credit risk of the company. Our joint valuation and estimation framework exploits this overlapping informational structure to provide better identification of the dynamics of the stock return variance and default arrival rate. The estimation results highlight the interrelated and yet distinct impacts of the two risk factors on the two types of derivative securities.

Also related to our work is a much longer list of studies on the linkages between the primary equity and debt markets. These studies can be classified into two broad approaches. The first is the structural modeling approach proposed by Merton (1974), who starts with a dynamic process (geometric Brownian motion) for the firm's asset value and treats the debt and equity of the firm as contingent claims on the firm's asset value.<sup>1</sup> The other approach is often termed as reduced-form, exemplified by another classic paper of Merton (1976), who recognizes the direct impact of corporate default on the stock price process and assumes that the stock price jumps to zero and stays there upon the random arrival of a default event.<sup>2</sup> Merton uses the first approach to analyze the company's capital structure and its impact on credit spreads, but he chooses the latter to analyze the impact of corporate

---

<sup>1</sup>Various modifications and extensions on the debt structure, default triggering mechanisms, firm value dynamics, and implementation procedures have been proposed in the literature. Prominent examples include Black and Cox (1976), Geske (1977), Ho and Singer (1982), Ronn and Verma (1986), Titman and Torous (1989), Kim, Ramaswamy, and Sundaresan (1993), Longstaff and Schwartz (1995), Leland (1994, 1998), Anderson and Sundaresan (1996), Anderson, Sundaresan, and Tychon (1996), Leland and Toft (1996), Briys and de Varenne (1997), Mella-Barral and Perraudin (1997), Garbade (1999), Fan and Sundaresan (2000), Duffie and Lando (2001), Goldstein, Ju, and Leland (2001), Zhou (2001), Acharya and Carpenter (2002), Huang and Huang (2003), Hull, Nelken, and White (2004), Bhamra, Kuehn, and Strebulaev (2007), Buraschi, Trojani, and Vedolin (2007), Chen, Collin-Dufresne, and Goldstein (2008), and Cremers, Driessen, and Maenhout (2008).

<sup>2</sup>Extensions and estimations of the jump-to-default-type models include Das and Sundaram (2004), Carr and Linetsky (2006), Le (2007), and Carr and Wu (2008b).

default on stock options pricing. Our work belongs to the latter approach as we focus on the dynamic linkages between the two (equity and credit) derivatives markets.

The remainder of this paper is organized as follows. The next section proposes a joint valuation framework for stock options and CDS. Section 2 describes the data set and summarizes the stylized evidence that motivates our specification. Section 3 describes the joint estimation procedure. Section 4 presents the results and discusses the implications. Section 5 concludes.

## 1 JOINT VALUATION OF STOCK OPTIONS AND CREDIT DEFAULT SWAPS

We consider a reference company that has positive probability of defaulting. Let  $P_t \geq 0$  denote the time- $t$  stock price for this company. We assume that the stock price  $P$  is strictly positive prior to default and falls to zero upon default. Let  $(\Omega, \mathcal{F}, (\mathcal{F}_t)_{t \geq 0}, \mathbb{Q})$  be a complete stochastic basis defined on the risk-neutral probability measure  $\mathbb{Q}$ . We assume that, prior to default, the company's stock price is governed by the following stochastic differential equation under the risk-neutral measure  $\mathbb{Q}$ ,

$$dP_t/P_{t-} = (r_t - q_t + \lambda_t)dt + \sqrt{v_t}dW_t^P + \int_{\mathbb{R}^0} (e^x - 1)(\mu(dx, dt) - \pi(x)dxv_tdt), \quad (1)$$

where  $P_{t-}$  denotes the time- $t$  pre-jump level of the stock price;  $r_t$  and  $q_t$  denote the instantaneous interest rate and dividend yield, respectively, which we assume evolve deterministically over time;  $\lambda_t$  denotes the risk-neutral arrival rate of the default event; and  $v_t$  denotes the instantaneous variance rate that controls the intensity of both the Brownian movement  $W_t^P$  and the jump movement in stock price prior to default. The incorporation of  $\lambda_t$  in the drift of the stock price process compensates for the possibility of a default, so that the forward price of the stock remains a martingale unconditionally under the risk-neutral measure.

The last term in Equation (1) under the integral denotes a jump martingale, with  $\mu(dx, dt)$  counting the number of jumps of size  $x$  and  $\pi(x)v_tdxdt$  being its compensator. The integral is over all possible jump sizes, defined on the whole real line excluding zero,  $\mathbb{R}^0$ . Conditional on the instantaneous variance rate level  $v_t$ , the arrival rate of jumps of size  $x$  is controlled by  $\pi(x)$ , which we specify as

$$\pi(x) = \begin{cases} \zeta e^{-x/v_+} x^{-1}, & x > 0 \\ \zeta e^{-|x|/v_-} |x|^{-1}, & x < 0, \end{cases} \quad (2)$$

where  $\zeta$  controls the average arrival rate scale and  $(v_+, v_-)$  control the average sizes of upside and downside jumps, respectively. With  $v_t$  fixed, the  $\pi(x)$  specification describes the variance-gamma Lévy jump process studied in Madan, Carr, and Chang (1998). In this model, the jump arrival rate declines monotonically as the absolute jump size declines. The singularity of the arrival rate at the origin leads to an infinite number of jumps within any finite time interval. We use this high-frequency jump component to describe the discontinuous stock price movements

during normal market conditions, in contrast to the rare, but catastrophic, default event that is controlled by a Cox process with arrival rate  $\lambda_t$ .

The pre-default stock price dynamics in Equation (1) is carefully specified to match the observed stock price behaviors. Several studies have found that high-frequency, infinite-activity jumps perform better than low-frequency, finite-activity jumps in capturing both the time-series behavior of stock and stock index returns (Carr et al., 2002; Li, Wells, and Yu, 2008) and the cross-sectional behavior of stock index options (Carr and Wu, 2003a; Huang and Wu, 2004). In line with such evidence, we include an infinite-activity jump component in the stock price dynamics.

Questions arise on whether a diffusion component is still needed once an infinite-activity jump is incorporated into the dynamics. In a pure Lévy setting, Carr et al. (2002) and Carr and Wu (2003a) find that it is difficult to identify a diffusion component in addition to an infinite-activity jump. On the other hand, Carr and Wu (2003b) construct a simple and robust test on the presence of jumps and diffusion components based on the asymptotic option price behavior as the option maturity approaches zero. They find that a diffusion component is always present and priced in the S&P 500 index options, whereas the additional contribution of a jump component varies over time. Recently, Todorov and Tauchen (2008) construct an activity signature function from discrete observations of a continuous process, and show that the asymptotic properties of the function as the sampling frequency increases can be used to make inferences on the activity behavior of the underlying process. Estimating the signature function on dollar/mark exchange rates, they also find supporting evidence for a diffusion component in addition to jumps. Hence, we specify a jump-diffusion instead of a pure jump specification.

We allow both the instantaneous variance rate  $v_t$  and the default arrival rate  $\lambda_t$  to be stochastic, and we model their joint dynamics under the risk-neutral probability measure  $\mathbb{Q}$  as

$$dv_t = (\theta_v - \kappa_v v_t) dt + \sigma_v \sqrt{v_t} dW_t^v, \quad (3)$$

$$\lambda_t = \beta v_t + z_t, \quad (4)$$

$$dz_t = (\theta_z - \kappa_z z_t) dt + \sigma_z \sqrt{z_t} dW_t^z, \quad \mathbb{E}[dW^z dW^P] = \mathbb{E}[dW^z dW^v] = 0 \quad (5)$$

$$\rho = \mathbb{E}[dW^P dW^v] / dt. \quad (6)$$

The specifications are motivated by both empirical evidence and economic justification. It is well documented that stock return volatility is stochastic. We use a square-root process in Equation (3) to model the dynamics of the instantaneous variance rate of the stock return prior to default. There is evidence that credit spreads of a company are positively related to the equity return volatilities of the same company.<sup>3</sup> Equation (4) captures this positive relation through a positive loading coefficient  $\beta$  between the default arrival rate  $\lambda_t$  and the variance rate  $v_t$ . It is also important to accommodate the reality that credit spreads sometimes move

<sup>3</sup>See, for example, Collin-Dufresne, Goldstein, and Martin (2001), Campbell and Taksler (2003), Bakshi, Madan, and Zhang (2006), Consigli (2004), and Zhu, Zhang, and Zhou (2005).

independent of the stock and stock options market. We use  $z_t$  to capture this independent credit risk component, with its dynamics controlled by an independent square-root process specified in (5). Finally, when the stock price falls, its return volatility often increases. A traditional explanation that dates back to Black (1976) is the leverage effect. So long as the face value of debt is not adjusted, a falling stock price increases the company's leverage and hence its risk, which shows up in stock return volatility.<sup>4</sup> Equation (6) captures this phenomenon via a negative correlation coefficient  $\rho$  between diffusion shocks in return and diffusion shocks in return variance.

### 1.1 Pricing Stock Options

Consider the time- $t$  value of a European call option  $c(P_t, K, T)$  with strike price  $K$  and expiry date  $T$ . The terminal payoff of the option is  $(P_T - K)^+$  if the company has not defaulted by that time, and is zero otherwise. The value of the call option can be written as

$$c(P_t, K, T) = \mathbb{E}_t \left[ \exp \left( - \int_t^T (r_s + \lambda_s) ds \right) (P_T - K)^+ \right], \quad (7)$$

where  $\mathbb{E}_t[\cdot]$  denotes the expectation operator under the risk-neutral measure  $\mathbb{Q}$  and conditional on the filtration  $\mathcal{F}_t$ . Given the deterministic interest rate assumption, we have

$$c(P_t, K, T) = B(t, T) \mathbb{E}_t \left[ \exp \left( - \int_t^T \lambda_s ds \right) (P_T - K)^+ \right] \quad (8)$$

with  $B(t, T)$  denoting the time- $t$  value of a default-free zero-coupon bond paying one dollar at its maturity date  $T$ . The expectation can be solved by inverting the following discounted generalized Fourier transform of the pre-default stock return,  $\ln(P_T/P_t)$ ,

$$\phi(u) \equiv \mathbb{E}_t \left[ \exp \left( - \int_t^T \lambda_s ds \right) e^{iu \ln(P_T/P_t)} \right], \quad u \in \mathcal{D} \subset \mathbb{C}, \quad (9)$$

where  $\mathcal{D}$  denotes the subset of the complex plane under which the expectation is well defined. Under the dynamics specified in Equations (1)–(6), the Fourier transform is exponential affine in the bivariate risk factor  $x_t \equiv [v_t, z_t]^\top$ :

$$\phi(u) = \exp(iu(r(t, T) - q(t, T))\tau - a(\tau) - b(\tau)^\top x_t), \quad \tau = T - t, \quad (10)$$

where  $r(t, T)$  and  $q(t, T)$  denote the continuously compounded spot interest rate and dividend yield at time  $t$  and maturity date  $T$ , respectively, and the

<sup>4</sup>Various other explanations have also been proposed in the literature; for example, Haugen, Talmor, and Torous (1991), Campbell and Hentschel (1992), Campbell and Kyle (1993), Bekaert and Wu (2000), and Carr and Wu (2008a).

time-homogeneous coefficients  $[a(\tau), b(\tau)]$  are given by

$$a(\tau) = \frac{\theta_v}{\sigma_v^2} 2 \ln 1 - \frac{\eta_v - \kappa_v^{\mathbb{M}}}{2\eta_v} (1 - e^{-\eta_v \tau}) + (\eta_v - \kappa_v^{\mathbb{M}}) \tau + \frac{\theta_z}{\sigma_z^2} 2 \ln 1 - \frac{\eta_z - \kappa_z}{2\eta_z} (1 - e^{-\eta_z \tau}) + (\eta_z - \kappa_z) \tau, \quad (11)$$

$$b(\tau) = \left[ \frac{2b_v(1 - e^{-\eta_v \tau})}{2\eta_v - (\eta - \kappa_v^{\mathbb{M}})(1 - e^{-\eta_v \tau})}, \frac{2b_z(1 - e^{-\eta_z \tau})}{2\eta_z - (\eta_z - \kappa_z)(1 - e^{-\eta_z \tau})} \right]^T \quad (12)$$

with  $\kappa_v^{\mathbb{M}} = \kappa_v - iu\sigma_v\rho$ ,  $\eta_v = \sqrt{(\kappa_v^{\mathbb{M}})^2 + 2\sigma_v^2 b_v}$ ,  $\eta_z = \sqrt{(\kappa_z)^2 + 2\sigma_z^2 b_z}$ ,  $b_z = 1 - iu$ , and  $b_v = (1 - iu)\beta + \frac{1}{2}(iu + u^2) + \zeta(\ln(1 - iuv_+)(1 + iuv_-) - iu \ln(1 - v_+)(1 + v_-))$ . Appendix A provides details of the derivation. Given  $\phi(u)$ , option prices can be obtained via fast Fourier inversion (Carr and Wu, 2004).

## 1.2 Pricing Credit Default Swap Spreads

The most actively traded credit derivative in the over-the-counter market is a CDS written on a corporate bond. The protection buyer pays a fixed premium, called the CDS spread, to the seller periodically over time. If a certain pre-specified credit event occurs, the protection buyer stops the premium payments and the protection seller pays the par value in return for the corporate bond. The CDS spread is set at inception so that the contract is costless to enter. As a result, the expected value of the premium payment leg is set equal to the expected value of the protection leg.<sup>5</sup>

Consider a CDS contract initiated at time  $t$  and with maturity date  $T$ . Let  $S(t, T)$  denote the fixed premium rate paid on this contract by the buyer of default protection. Assuming one dollar notional and continuous payments for simplicity, we can write the present value of the premium leg of the contract as

$$\text{Premium}(t, T) = \mathbb{E}_t \left[ S(t, T) \int_t^T \exp \left( - \int_t^s (r_u + \lambda_u) du \right) ds \right] \quad (13)$$

with  $r$  and  $\lambda$  denoting the instantaneous benchmark interest rate and default arrival rate. Further, assuming that upon default, the underlying corporate bond recovers a fixed fraction  $w$  of its par value, we can write the present value of the protection leg as

$$\text{Protection}(t, T) = \mathbb{E}_t \left[ (1 - w) \int_t^T \lambda_s \exp \left( - \int_t^s (r_u + \lambda_u) du \right) ds \right]. \quad (14)$$

<sup>5</sup>For companies with high default probabilities, the industry often switches to another convention, under which the protection buyer pays an upfront fee to the protection seller with the periodic premium payment fixed at 500 basis points per annum of the notional amount. At the time of this writing, the North America CDS market is going through further reforms to increase the fungibility and to facilitate central clearing of the contracts. The convention on virtually all contracts is switching to fixed premium payments of either 100 or 500 basis points, with upfront fees to settle the value differences between the two legs.

By equating the present values of the two legs, we can solve for the CDS spread  $S(t, T)$  that sets the contract value to zero at initiation:

$$S(t, T) = \frac{\mathbb{E}_t (1 - w) \int_t^T \lambda_s \exp \left( - \int_t^s (r_u + \lambda_u) du \right) ds}{\mathbb{E}_t \int_t^T \exp \left( - \int_t^s (r_u + \lambda_u) du \right) ds}, \quad (15)$$

which can be regarded as a weighted average of the expected default loss.

Under the dynamics specified in Equations (3)–(6), we can solve for the present values of the two legs of the CDS. The value of the premium leg can be written as

$$\text{Premium}(t, T) = S(t, T) \int_t^T B(t, s) \mathbb{E}_t \left[ \exp \left( - \int_t^s b_{\lambda 0}^\top x_u du \right) \right] ds \quad (16)$$

with  $b_{\lambda 0} = [\beta, 1]^\top$ . The affine dynamics for the bivariate risk factors  $x$  and the linear loading function  $b_{\lambda 0}$  dictate that the present value of the premium leg is an exponential affine function of the state vector (Duffie, Pan, and Singleton, 2000):

$$\text{Premium}(t, T) = S(t, T) \int_t^T B(t, s) \exp \left( - a_\lambda(s - t) - b_\lambda(s - t)^\top x_t \right) ds, \quad (17)$$

where the affine coefficients can be solved analytically:

$$a_\lambda(\tau) = \frac{\theta_v}{\sigma_v^2} \left[ 2 \ln \left( 1 - \frac{\eta_v - \kappa_v}{2\eta_v} (1 - e^{-\eta_v \tau}) \right) + (\eta_v - \kappa_v) \tau \right] \\ + \frac{\theta_z}{\sigma_z^2} \left[ 2 \ln \left( 1 - \frac{\eta_z - \kappa_z}{2\eta_z} (1 - e^{-\eta_z \tau}) \right) + (\eta_z - \kappa_z) \tau \right], \quad (18)$$

$$b_\lambda(\tau) = \frac{2\beta(1 - e^{-\eta_v \tau})}{2\eta_v - (\eta_v - \kappa_v)(1 - e^{-\eta_v \tau})}, \quad \frac{2(1 - e^{-\eta_z \tau})}{2\eta_z - (\eta_z - \kappa_z)(1 - e^{-\eta_z \tau})}^\top \quad (19)$$

with  $\eta_v = \sqrt{(\kappa_v)^2 + 2\sigma_v^2\beta}$  and  $\eta_z = \sqrt{(\kappa_z)^2 + 2\sigma_z^2}$ .

The present value of the protection leg can be written as

$$\text{Protection}(t, T) = (1 - w) \int_t^T B(t, s) \mathbb{E}_t \left[ b_{\lambda 0}^\top x_s \exp \left( - \int_t^s b_{\lambda 0}^\top x_u du \right) \right] ds, \quad (20)$$

which also allows for an affine solution

$$\text{Protection}(t, T) = (1 - w) \int_t^T B(t, s) (c_\lambda(s - t) + d_\lambda(s - t)^\top x_t) \\ \times \exp(-a_\lambda(s - t) - b_\lambda(s - t)^\top x_t) ds, \quad (21)$$

where the coefficients  $(a_\lambda(\tau), b_\lambda(\tau))$  are the same as in (17), and the coefficients  $(c_\lambda(\tau), d_\lambda(\tau))$  can also be solved analytically by taking partial derivatives against  $(a_\lambda(\tau), b_\lambda(\tau))$  with respect to maturity  $\tau$ :

$$c_\lambda(\tau) = \partial a_\lambda(\tau) / \partial \tau, \quad d_\lambda(\tau) = \partial b_\lambda(\tau) / \partial \tau. \quad (22)$$



**Table 1** List of companies.

Equity ticker	Company name	Sector	Credit rating <sup>a</sup>
C	Citigroup Inc.	Financial	AA
DUK	Duke Energy Corporation	Utilities	BBB
F	Ford Motor Company	Consumer Cyclical	BB
FNM	Fannie Mae	Financial	AAA
GM	General Motors Corporation	Consumer Cyclical	B
IBM	International Business Machines Corp	Services	A
MO	Altria Group, Inc.	Consumer Non-Cyclical	BBB
T	AT&T Inc.	Services	A/BBB

<sup>a</sup>During our sample period, from May 2002 to May 2006.

Combining the solutions for the present values of the two legs in Equations (16) and (21) leads to the CDS spread  $S(t, T)$ . When we estimate the model, we discretize the above equation to accommodate quarterly premium payments.

### 1.3 Market Prices of Risks and Time-Series Dynamics

Our estimation procedure identifies both the time-series dynamics and the risk-neutral dynamics of the bivariate state vector  $x_t = [v_t, z_t]^T$ . To derive the time-series dynamics for the bivariate vector  $x_t$  under the statistical measure  $\mathbb{P}$ , we assume that the market prices of risks are proportional to the corresponding risk level. Under this assumption, the time-series dynamics are

$$dv_t = \theta_v - \kappa_v^{\mathbb{P}} v_t dt + \sigma_v \sqrt{v_t} dW_t^v, \quad dz_t = \theta_z - \kappa_z^{\mathbb{P}} z_t dt + \sigma_z \sqrt{z_t} dW_t^z, \quad (23)$$

where  $\kappa_v^{\mathbb{P}} = \kappa_v - \sigma_v \gamma_v$  and  $\kappa_z^{\mathbb{P}} = \kappa_z - \sigma_z \gamma_z$ , with  $(\gamma_v, \gamma_z)$  denoting the two proportional market price of risk coefficients on the two risk sources  $(W^v, W^z)$ .

## 2 DATA AND EVIDENCE

We collect data on CDS spreads and stock option prices for eight reference companies from May 8, 2002 to May 10, 2006. The choices of the sample period and the company list are largely determined by data availability and coverage. The eight companies are Citigroup Inc. (C), Duke Energy Corporation (DUK), Ford Motor Company (F), Fannie Mae (FNM), General Motors Corporation (GM), International Business Machines Corp (IBM), Altria Group, Inc. (MO), and AT&T Inc. (T). Table 1 lists the eight companies, including their equity tickers, company names, the sectors that they belong to, and their credit ratings during our four-year sample period. The eight companies span six major rating classes from B to AAA, and cover five different sectors including Financials, Utilities, Consumer Cyclical,

Services, and Consumer Non-Cyclicals. Thus, the eight companies that we choose cover a wide spectrum of credit ratings and industry sectors.

## 2.1 Data Description

We obtain the CDS spread quotes from several broker dealers. We cross-validate the numbers and take the quotes from the most reliable source. The constructed dataset includes six time series for each company at six fixed terms: one, two, three, five, seven, and 10 years.

The stock options data are from OptionMetrics. Exchange-traded options on individual stocks are American-style and hence the price reflects an early exercise premium. OptionMetrics uses a binomial tree to back out the option implied volatility that explicitly accounts for this early exercise premium. We estimate our model specification based on their implied volatility estimates. At each time and maturity, we take the implied volatility quotes of out-of-the-money options (call options when the strike is higher than the spot, and put options when strike is lower than the spot) and convert them into European option values based on the Black and Scholes (1973) pricing formula.

Processing the options data involves careful considerations and delicate choices. Normally, two options are available at each maturity and strike: one call and the other put. For European options, put-call parity dictates that the put and the call at the same maturity and strike have the same time value and thus the same implied volatility. For model estimation, it suffices to pick one of them as the two options contain identical information about the underlying stock price dynamics. When the two options quotes deviate from put-call parity due to measurement errors or market frictions (such as short-sale constraints), taking a weighted average of the time values or implied volatilities of the two options can be a useful way to reduce measurement noise. Since out-of-the-money options are more actively traded than in-the-money options, the quotes on out-of-the-money options are usually more reliable. Thus, the weight should be higher on the out-of-the-money option than on its in-the-money counterpart. The exact weighting scheme becomes an empirical issue and can vary across markets.

The American feature of the single name options adds another layer of complexity. Directly using the model to generate American values is numerically difficult and computationally intensive. A commonly used shortcut is to extract the Black-Scholes implied volatility from the price of an American option and use the implied volatility to compute a European option value for the same maturity date and strike. Put-call parity does not hold for American options, nor does it need to hold for the European option values that we computed from the American option prices. Apart from measurement errors and market frictions, in-the-money options often have a higher chance of being exercised early and hence have a shorter effective maturity—A ten-year option to be exercised tomorrow only has an effective maturity of one day left. The implied volatility estimate on each option reflects the volatility over the effective maturity horizon. Thus, when the implied volatility has a nonflat term structure, the two implied volatility estimates from

the American put and call will not be the same. In this case, we choose to use the out-of-the-money option implied volatility except for near-the-money contracts.<sup>6</sup> As discussed earlier, out-of-the-money options are more actively traded and the quotes are usually more reliable. Furthermore, for American options, the effective maturity of the out-of-the-money option is closer to the maturity of the contract. Thus, the de-Americanization procedure introduces smaller approximation errors for out-of-the-money options.

To price the CDS contracts and to convert the implied volatility into option values, we also need the underlying interest rate curve. Following standard industry practice, we use the interest rate curve defined by the Eurodollar LIBOR and swap rates. We download LIBOR rates at maturities of one, two, three, six, nine, and 12 months and swap rates at two, three, four, five, seven, and 10 years. We use a piecewise constant forward function in bootstrapping the discount rate curve.

## 2.2 Summary Statistics of CDS Spreads

Table 2 reports the summary statistics of the CDS spreads on the eight reference companies. Panel A reports the sample averages of the CDS spreads at each of the six maturities and for each of the eight companies. At each maturity, the average spread varies greatly across the eight reference names. The average spread is the lowest for the AAA-rated Fannie Mae, followed by AA-rated Citigroup and then by A-rated IBM. The average spreads on these A-level companies are less than 50 basis points across all six maturities. The next group are the BBB-rated companies, including Duke Energy, Altria, and AT&T, with the credit spreads averaging between 50 and 200 basis points. Finally, BB-rated Ford and B-rated General Motors have much higher average spreads over our sample period, ranging from three to five percentage points. For all eight companies, the average spreads at long maturities are much higher than the average spreads at short maturities. The differences generate steeply upward sloping mean term structures on the CDS spreads.

Panel B of Table 2 reports the standard deviation estimates on the CDS spread series. The standard deviation estimates are similar in magnitude to the average spreads, suggesting large historical variations on each series. The only exception is the spread on Fannie Mae, the standard deviation estimates of which are much smaller than the already low mean spread estimates. We conjecture that the implicit government guarantee on the agency debt not only lowers the credit spread level, but also makes the spread stable over time.

The term structures of the standard deviations show different shapes for different companies, upward sloping for the three high-rating companies C, FNM, and IBM, downward sloping for DUK, GM, MO, and T, and hump-shaped for F. If the credit spread were driven by one strongly mean-reverting risk factor, we would expect the standard deviations to be lower at longer maturities and hence

---

<sup>6</sup>We apply equal weight to the two at-the-money implied volatilities, but let the weight decline rapidly as the option becomes in-the-money.

**Table 2** Summary statistics of credit default swap spreads.

Years	CDS spreads, in basis points							
	C	DUK	F	FNM	GM	IBM	MO	T
Panel A: Mean								
1	0.136	0.566	2.885	0.094	3.527	0.193	1.352	1.469
2	0.169	0.602	3.717	0.122	4.220	0.228	1.461	1.629
3	0.203	0.601	4.087	0.152	4.592	0.261	1.539	1.680
5	0.275	0.700	4.442	0.216	4.787	0.335	1.602	1.868
7	0.327	0.749	4.476	0.259	4.776	0.398	1.675	1.965
10	0.401	0.847	4.492	0.308	4.783	0.489	1.769	2.075
Panel B: Standard deviation								
1	0.118	0.659	2.395	0.048	4.211	0.178	1.122	1.980
2	0.131	0.660	2.653	0.052	4.393	0.175	1.027	1.897
3	0.141	0.490	2.668	0.055	4.210	0.191	0.950	1.688
5	0.150	0.460	2.538	0.059	3.732	0.199	0.756	1.567
7	0.151	0.416	2.428	0.056	3.482	0.188	0.699	1.473
10	0.156	0.482	2.315	0.058	3.335	0.198	0.656	1.399
Panel C: Autocorrelation								
1	0.976	0.828	0.975	0.957	0.978	0.970	0.906	0.981
2	0.981	0.897	0.973	0.962	0.979	0.982	0.930	0.975
3	0.982	0.940	0.971	0.954	0.978	0.979	0.932	0.981
5	0.980	0.949	0.971	0.951	0.979	0.977	0.934	0.979
7	0.978	0.951	0.971	0.929	0.980	0.978	0.926	0.979
10	0.974	0.826	0.970	0.906	0.979	0.969	0.925	0.973

The statistics are based on weekly sampled data (every Wednesday) from May 8, 2002 to May 10, 2006; 210 observations for each series.

the standard deviation term structure to be downward sloping. The different term structure shapes observed in CDS spreads suggest that credit risk factors can be highly persistent under the risk-neutral measure. Panel C of Table 2 shows that the weekly autocorrelation estimates on the CDS spreads are also very high, ranging from 0.826 to 0.982. The high estimates suggest that the CDS spreads (and hence credit risk factors) are also highly persistent under the statistical measure.

Figure 1 plots the time series of CDS spreads at selected maturities of one year (solid lines), five years (dashed lines), and 10 years (dash-dotted lines). Each panel is for one company. Seven of the eight chosen companies have experienced dramatic credit spread variations during our sample period. The CDS spreads have spiked for these companies at least once during our sample period. The one exception is Fannie Mae, which shows the stabilizing effect of the implicit government guarantee. The three lines in each panel also reveal the CDS term structure and its variations. The long-term CDS spreads are on average wider than the short-term CDS spreads, especially during calm periods; but the term structure can become downward sloping when the CDS spread level spikes.

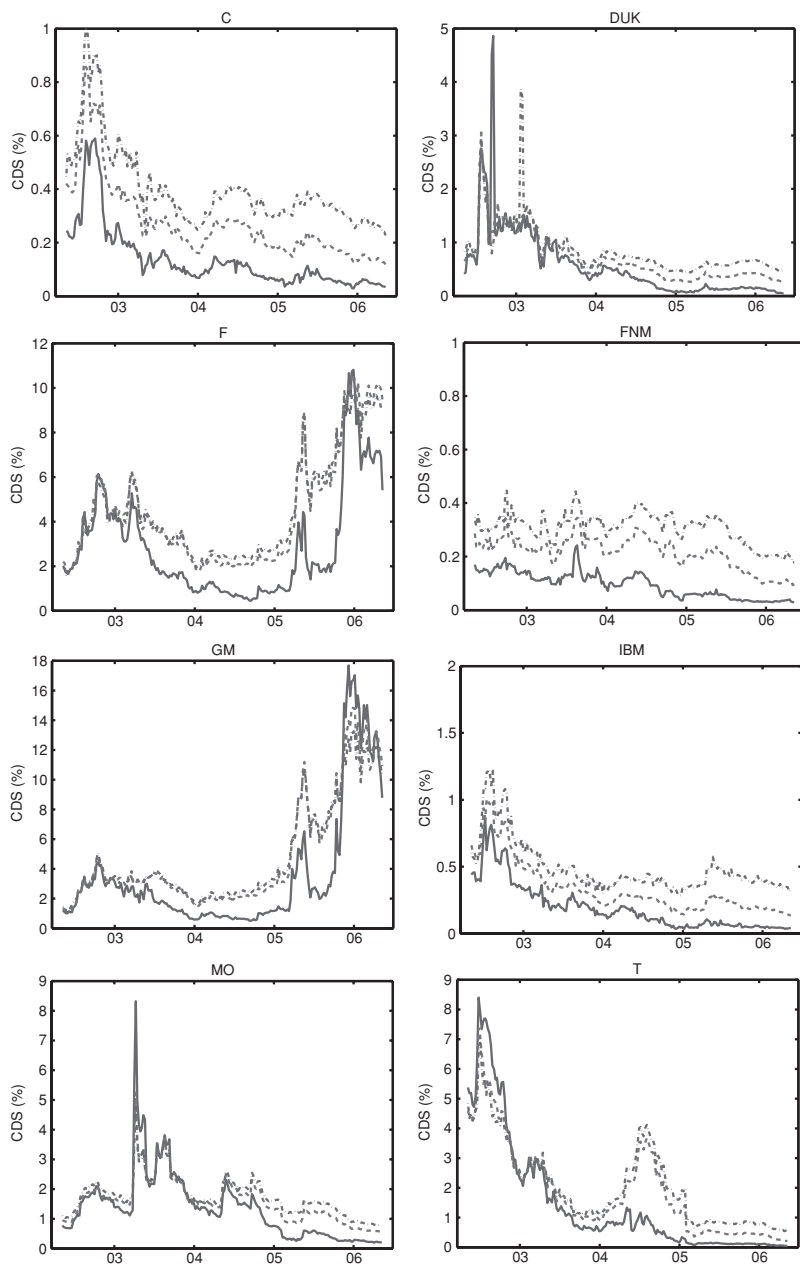


**Figure 1** The time series of CDS spreads at selected maturities of one year (solid lines), five years (dashed lines), and 10 years (dash-dotted lines). Each panel is for one company.

### 2.3 Summary Statistics of Stock Option Implied Volatilities

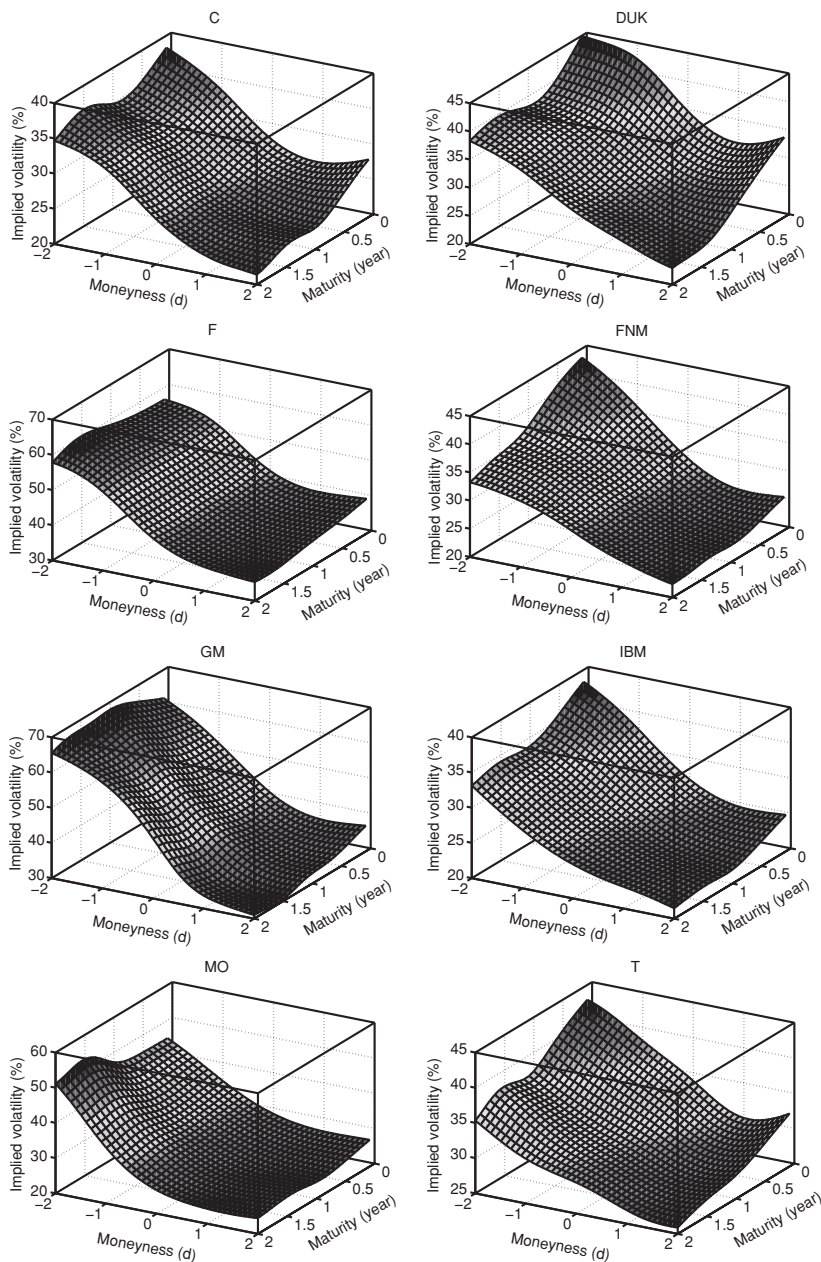
The exchange-listed stock options are quoted at fixed strike prices and expiration dates. As calendar time passes and the underlying stock price changes, the moneyness and time-to-maturity of each contract also change. To analyze the cross-sectional behavior of the options across different levels of moneyness and maturity, we perform nonparametric regressions on the option implied volatilities against the time to maturity ( $\tau$ ) and a standardized moneyness measure  $d \equiv \ln(K/P_i)/(IV\sqrt{\tau})$ , where  $K$  denotes the strike price and  $IV$  denotes the Black–Scholes implied volatility of the option. We perform nonparametric regression using an independent bivariate Gaussian kernel and a default choice of bandwidth that is proportional to  $\sigma_x N^{-1/6}$ , with  $N$  being the number of observations and  $\sigma_x$  being the standard deviation of the regressor  $x$ .

Figure 2 plots the nonparametrically estimated mean implied volatility surface for the eight companies, one company in each panel. Compared to the large cross-sectional variation of the average CDS spreads across the eight companies, the average implied volatility levels vary within a narrower range of 20%–70%. The eight mean implied volatility surfaces also share similar shapes. The mean implied volatility exhibits the well-documented smile pattern along the moneyness dimension at short maturities, but this smile gradually becomes a negatively sloped skew at longer maturities.<sup>7</sup> It has been well appreciated that the implied volatility smiles and skews along the moneyness direction are direct results of conditional non-normality in the underlying stock returns under the risk-neutral measure. The positive curvature of the smile reflects fat tails (positive excess kurtosis) in the risk-neutral return distribution, whereas the negative slope of the implied volatility skew indicates negative skewness in the risk-neutral return distribution. Under our model specification, negative risk-neutral return skewness can come from three sources: (i) positive probability of default ( $\lambda > 0$ ), (ii) asymmetry in the high-frequency jump component ( $v_- > v_+$ ), and (iii) negative correlation between the return Brownian motion component and its instantaneous variance rate ( $\rho < 0$ ).

To analyze the time-series behavior of implied volatility, we interpolate to create implied volatility estimates at fixed levels of moneyness and maturity at each date. We first perform a local quadratic regression of the implied variance on the standard moneyness measure  $d$  at each observed maturity and date. The local quadratic regression generates not only the interpolated implied variance, but also the slope and curvature estimates of the locally quadratic fit at each moneyness point. Then, at each fixed moneyness level, we perform linear interpolation along the maturity dimension on the total variance and the implied variance slope to generate the implied variance and the implied variance skew at fixed maturities.

Table 3 reports the summary statistics of the interpolated implied volatility time series at selected moneyness levels and maturities. We choose two maturities,

<sup>7</sup>Dennis and Mayhew (2002) and Bakshi, Kapadia, and Madan (2003) have examined the negative skew of the implied volatility plot for individual stock options.



**Figure 2** Mean implied volatility surface across moneyness and time to maturity. The mean implied volatility surface as a function of time to maturity  $\tau$  and a standardized moneyness measure  $d$  is estimated nonparametrically with an independent bivariate Gaussian kernel. Each panel represents one company.

**Table 3** Summary statistics of interpolated implied volatility series.

Days	Implied volatilities, in percentages								
	$d$	C	DUK	F	FNM	GM	IBM	MO	T
Panel A: Mean									
30	−1	29.824	35.612	49.636	34.407	45.991	28.806	33.043	33.078
30	0	24.623	28.965	40.640	28.115	37.725	24.594	27.342	28.294
30	1	22.414	27.007	38.038	25.354	34.733	23.256	26.021	25.815
360	−1	30.873	35.751	51.194	34.390	52.742	29.116	34.660	31.994
360	0	24.878	28.685	40.160	27.725	38.767	24.429	27.179	27.483
360	1	21.150	25.434	35.371	23.548	29.808	21.604	23.703	24.422
Panel B: Standard deviation									
30	−1	15.587	20.607	15.462	8.296	19.377	13.057	9.924	15.456
30	0	12.322	15.578	11.740	6.035	14.491	10.274	7.638	12.919
30	1	10.445	13.061	9.909	4.625	12.062	8.488	6.404	11.954
360	−1	10.037	16.309	13.536	5.228	20.755	9.369	5.977	10.619
360	0	8.229	11.731	10.393	3.422	14.381	7.760	4.336	8.802
360	1	6.650	9.341	8.017	2.399	7.829	6.392	3.884	7.942
Panel C: Autocorrelation									
30	−1	0.943	0.949	0.927	0.871	0.932	0.960	0.788	0.909
30	0	0.939	0.941	0.908	0.838	0.927	0.951	0.753	0.928
30	1	0.929	0.947	0.900	0.817	0.924	0.937	0.753	0.942
360	−1	0.980	0.976	0.957	0.942	0.974	0.989	0.915	0.985
360	0	0.979	0.975	0.956	0.926	0.969	0.987	0.914	0.984
360	1	0.974	0.974	0.956	0.899	0.952	0.983	0.931	0.983

Entries report the sample estimates of the mean, standard deviation, and weekly autocorrelation on interpolated implied volatility series at selected fixed moneyness levels and maturities. We first perform a local quadratic nonparametric regression of the implied variance on moneyness to obtain implied variance at fixed moneyness levels for observed maturities. The moneyness of each option is defined as  $d \equiv \ln(K/P_t)/(IV\sqrt{\tau})$ , where  $K$  denotes the strike,  $P_t$  the stock price level,  $IV$  the implied volatility estimate, and  $\tau$  the time to maturity. Then, at each fixed moneyness level, we interpolate across the maturity dimension using piecewise linear interpolation on the total variance. The statistics on the interpolated series are based on weekly sampled data (every Wednesday) from May 8, 2002 to May 10, 2006; 210 observations for each series.

one at the short end at one month (30 days), and the other at the long end at one year (360 days). At each of the two maturities, we choose three moneyness levels at  $d = -1, 0, 1$ . Approximately speaking,  $d = -1$  corresponds to a strike that is one standard deviation below the current spot price level and  $d = 1$  corresponds to a strike that is one standard deviation above the current spot price level. Panel A reports the sample average of the implied volatility levels. The average implied volatility levels are mostly in the range of 20%–50%, with the averages for BB-rated Ford and B-rated General Motors higher than the averages for the other companies with higher credit ratings. At each maturity and for each company, the average implied volatility at  $d = -1$  is higher than the average implied



**Table 4** Co-movements of credit spreads with stock option implied volatilities and implied variance skews.

Days	$d$	C	DUK	F	FNM	GM	IBM	MO	T
Panel A: Implied volatility									
30	-1	0.177	0.457	0.424	0.157	0.498	0.223	0.560	0.134
30	0	0.147	0.449	0.370	0.146	0.450	0.200	0.482	0.110
30	1	0.145	0.435	0.395	0.169	0.438	0.183	0.411	0.113
360	-1	0.257	0.536	0.590	0.244	0.786	0.307	0.711	0.257
360	0	0.269	0.540	0.577	0.257	0.774	0.310	0.618	0.175
360	1	0.248	0.469	0.558	0.250	0.646	0.298	0.462	0.103
Panel B: Negative implied variance skew									
30	-1	0.183	0.469	0.286	0.076	0.488	0.287	0.674	0.103
30	0	0.169	0.475	0.293	0.096	0.490	0.309	0.667	0.085
30	1	0.151	0.492	0.304	0.050	0.470	0.262	0.649	0.055
360	-1	0.235	0.451	0.504	0.195	0.762	0.235	0.817	0.259
360	0	0.232	0.462	0.493	0.204	0.758	0.250	0.817	0.225
360	1	0.247	0.460	0.370	0.176	0.723	0.188	0.698	0.146

Entries report the cross-correlation estimates between weekly changes in the average CDS spreads for each company and weekly changes in the stock option implied volatility (panel A) and the negative of the implied variance skew (panel B) across different maturities and moneyness. We use a simple average of the six CDS series as an average credit spread series for each company. To obtain the implied volatility and skew series at fixed time to maturities and moneyness, we first perform a local quadratic regression of the implied variance on the moneyness  $d$  to obtain implied variance and its slope at fixed moneyness levels for observed maturities. Then, at each fixed moneyness level, we linearly interpolate on total variance and the skew to obtain the implied variance and skew at fixed time to maturities. The statistics are based on weekly sampled data (every Wednesday) from May 8, 2002 to May 10, 2006; 210 observations for each series.

volatility at  $d = 1$ , consistent with the negatively sloped skew observed in Figure 2. At each fixed moneyness, the average implied volatility does not show much variation across the two maturities. By contrast, the standard deviation estimates reported in panel B show significantly smaller magnitudes at longer maturities. The downward sloping variance standard deviation term structure is consistent with mean-reverting variance risk dynamics under the risk-neutral measure. The last panel (panel C) in Table 3 reports the weekly autocorrelation estimates of the implied volatility series. The estimates are high, suggesting that the implied volatility series are highly persistent in their time-series dynamics.

## 2.4 Co-Movements between Option Implied Volatilities and CDS Spreads

To analyze how a company's CDS spreads co-move with the company's stock options, Table 4 measures the cross-correlation of the weekly changes in the average CDS spread for a company with weekly changes in the stock option implied volatility levels (panel A) and the implied variance skews (panel B) of the same

company at different levels of moneyness and maturity. For each company and at each date, we use a simple average of the six CDS quotes at the six maturities to represent the average CDS spread for the company.

The estimates in panel A show that the correlations between the credit spreads and the stock option implied volatilities are universally positive across all companies, all maturities, and all moneyness levels. For each company, the correlation estimates are in general higher at low strikes ( $d = -1$ ) than at high strikes ( $d = 1$ ). The estimates are also higher at one year than at one month maturities. Under our model specification, this positive correlation can come from two major sources. First, the positive loading coefficient  $\beta$  in Equation (4) generates a direct positive linkage between stock return variance and the default arrival rate. Second, the default arrival rate itself contributes positively to the option implied volatility.

The implied variance skew estimates are predominantly negative, especially at long maturities and low strikes. Panel B of Table 4 reports the correlation estimates between weekly changes in the credit spread and weekly changes in the negative of the implied variance skew at different maturities and moneyness. The estimates are again universally positive, suggesting that when a company's credit spread widens, its implied variance skew becomes more negatively skewed. Overall, the implied variance skew at longer maturities show higher correlation with the credit spread.

In Figure 3, we overlay the time series of the average CDS spread (solid line) with the one-year stock option implied volatility at  $d = 0$  (dashed line) and the negative of the one-year implied variance skew at  $d = 0$  (dash-dotted line), one panel for each company. To accommodate the scale differences in the same plot, we normalize each time series to have unit sample standard deviation. The comparative time-series plots show that for each company, the CDS series show positive co-movements with both the implied volatility and the implied variance skew time series. They also show variations independent of one another.

Both the correlation estimates in Table 4 and the time-series plots in Figure 3 show that the credit spread is intricately related to the equity options market. The linkages ask for a dynamically and internally consistent theoretical framework to jointly model the dynamics and pricing of default arrival rates and stock return variance. Our model does just that, and it accommodates both the positive co-movements and their separate variations through the bivariate specifications in Equations (3)–(5).

### 3 JOINT ESTIMATION OF MARKET AND CREDIT RISK DYNAMICS

We estimate the bivariate risk dynamics  $x_t = [v_t, z_t]^\top$  jointly using both CDS spreads and stock options. We cast the model into a state-space form and estimate the model using a quasi-maximum likelihood method.

In the state-space form, we regard the bivariate risk vector as the unobservable states and specify the state propagation equation as an Euler approximation of the

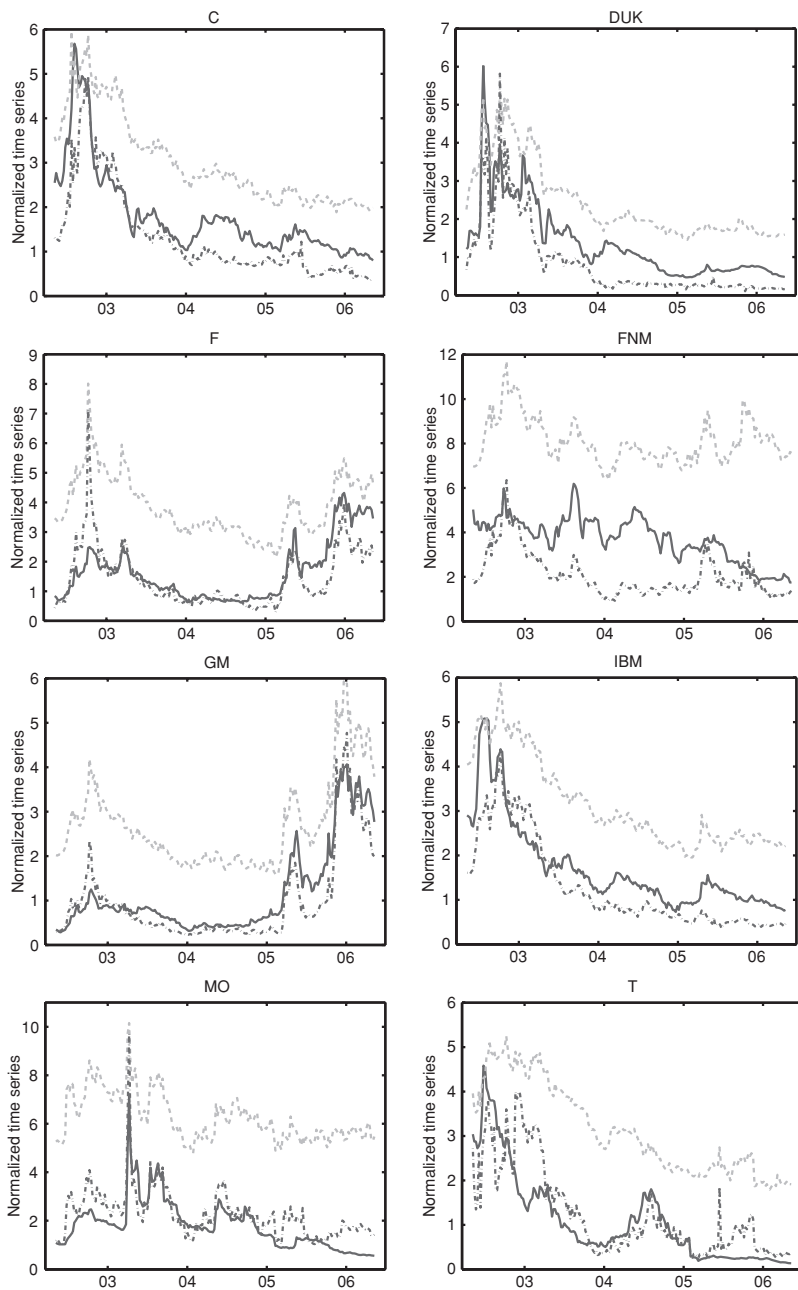


**Figure 3** Co-movements of CDS spreads with stock option implied volatilities and implied variance skews. Each panel represents one company. The three lines in each panel denote the normalized time series of the average CDS spreads (solid lines), the one-year implied volatilities (dashed lines), and the negative of the implied variance skew (dash-dotted lines). Each time series is normalized to have unit sample standard deviation.

time-series dynamics in Equation (23):

$$x_t = \begin{bmatrix} \theta_v \\ \theta_z \end{bmatrix} \Delta t + \begin{bmatrix} e^{-\kappa_v^P \Delta t} & 0 \\ 0 & e^{-\kappa_z^P \Delta t} \end{bmatrix} x_{t-1} + \sqrt{\begin{bmatrix} \sigma_v^2 v_{t-1} \Delta t & 0 \\ 0 & \sigma_z^2 z_{t-1} \Delta t \end{bmatrix}} \varepsilon_t, \quad (24)$$

where  $\varepsilon$  denotes an iid bivariate standard normal innovation and  $\Delta t = 7/365$  denotes the sampling frequency.

We construct the measurement equation based on CDS spreads and stock options, assuming additive, normally distributed measurement errors

$$y_t = h(x_t; \Theta) + e_t, \quad (25)$$

where  $y_t$  denotes the observed series and  $h(x_t; \Theta)$  denotes the corresponding model value as a function of the state vector  $x_t$  and model parameters  $\Theta$ . Each day, the measurement equation contains six CDS spread quotes at six different maturities. We scale each CDS series by its sample average and then assume that the pricing errors on the six scaled CDS series are iid normal with variance  $\sigma_C^2$ . The number of option observations varies across different dates and different companies. The estimation includes options with a minimum of 10 days to expiration and strike prices within two standard deviations of the spot ( $|d| \leq 2$ ). The average number of options per day included in the estimation ranges from 25 for Ford to 59 for General Motors. The option maturity for each company ranges from the minimum requirement of 10 days to about 2.5 years, with the median maturity varying from 190 to 290 days for different companies. We scale the out-of-the-money European option values at each strike price and maturity by its Black–Scholes vega, and assume that the scaled pricing errors on all options are iid normal with variance  $\sigma_O^2$ .

When both the state propagation equation and the measurement equation are Gaussian and linear, the Kalman (1960) filter generates efficient forecasts and updates on the conditional mean and covariance of the state vector and the measurement series. In our application, the state propagation equation in (24) is Gaussian and linear, but the measurement equation in (25) is nonlinear. We use the unscented Kalman filter (Wan and van der Merwe, 2001) to handle the nonlinearity. The unscented Kalman filter approximates the posterior state density using a set of deterministically chosen sample points (sigma points). These sample points completely capture the mean and covariance of the Gaussian state variables, and when propagated through the nonlinear functions in the measurement equation, capture the posterior mean and covariance of the CDS spreads and option prices accurately to the second order for any nonlinearity. Appendix B provides the technical details for the filtering methodology.

We construct the log-likelihood value assuming normally distributed forecasting errors. Furthermore, since we use different numbers of options and CDS spreads in the estimation, the estimated dynamics tend to bias toward the market with more data observations. To correct for this bias and to assign approximately equal weights to both markets, we separately calculate the weekly likelihood

values on the options ( $l_t^O$ ) and the CDS spreads ( $l_t^C$ ), and we divide the two likelihood values by the number of option ( $n_t^O$ ) and CDS ( $n_t^C$ ) observations in that week, respectively. Then, we maximize the sum of the rescaled log-likelihood values over the whole data series to estimate the model parameters:

$$\Theta \equiv \arg \max_{\Theta} \sum_{t=1}^N l_t^C(\Theta)/n_t^C + l_t^O(\Theta)/n_t^O, \quad (26)$$

where  $\Theta$  denotes 16 model parameters to be estimated:  $\Theta \equiv [\kappa_v, \kappa_z, \kappa_v^{\mathbb{P}}, \kappa_z^{\mathbb{P}}, \theta_v, \theta_z, \sigma_v, \sigma_z, \beta, \rho, \zeta, v_+, v_-, w, \sigma_C^2, \sigma_O^2]^{\top}$  and  $N = 210$  denotes the number of weeks in our sample.

## 4 RESULTS AND DISCUSSION

First, we summarize the performance of our joint valuation model on CDS spreads and stock options on the eight reference companies. Then, from the estimates of the model parameters, we discuss the joint dynamics and pricing of the return variance risk and default arrival risk, and their impacts on the CDS spread term structure and the option implied volatility surface.

### 4.1 Performance Analysis

Table 5 reports the summary statistics of the pricing errors on the credit default swap spreads and option implied volatilities. We report the pricing errors on the CDS spreads at each of the six fixed terms and the pricing errors on the implied volatilities as one pooled series for each company. The pricing errors are defined as the differences between the data observations (CDS spreads and option implied volatilities, both in percentage points) and the corresponding model values.

Panel A of Table 5 reports the sample averages of the pricing errors. The mean pricing errors for the CDS spreads do not show any obvious structure, except for Altria and AT&T, where the mean errors show a positive mean bias across all maturities. The mean bias is about 5–10 basis points for Altria and 12–26 basis points for AT&T. The mean biases on the option implied volatilities are all positive but small, less than half a volatility percentage point for all companies, and less than one-tenth of a volatility point for Altria and AT&T.

To learn how the mean option pricing errors vary across the option moneyness and maturity spectrum, we perform nonparametric regressions on the pricing errors as a function of moneyness  $d$  and maturity, using the same methodology as we have done to obtain the mean implied volatility surface in Figure 2. Figure 4 plots the mean pricing error surfaces, one panel for each company. The shapes of the mean pricing error surface vary across different reference companies, with no systematic pattern. The largest mean pricing errors come from Altria and AT&T, with the mean errors negative at low strikes (negative  $d$ ), but positive at high strikes (positive  $d$ ). The biases are stronger at longer maturities. The mean bias pattern across the moneyness dimension suggests that the observed implied volatilities are not as negatively skewed as the model-implied values. Under our model

**Table 5** Summary statistics of pricing errors on CDS spreads and option implied volatilities.

	C	DUK	F	FNM	GM	IBM	MO	T
Panel A: Mean pricing errors								
1	−0.003	−0.030	−0.285	−0.005	−0.140	−0.002	0.102	0.124
2	−0.003	−0.052	0.226	−0.004	0.222	−0.003	0.104	0.175
3	−0.001	−0.095	0.319	−0.000	0.335	−0.006	0.100	0.135
5	0.010	−0.043	0.245	0.013	0.187	−0.000	0.052	0.195
7	0.003	−0.016	−0.016	0.008	−0.015	0.001	0.062	0.212
10	−0.005	0.068	−0.272	−0.011	−0.153	0.011	0.104	0.257
IV	0.308	0.396	0.259	0.244	0.360	0.278	0.015	0.076
Panel B: Mean absolute pricing errors								
1	0.014	0.175	0.524	0.008	0.417	0.020	0.139	0.337
2	0.009	0.179	0.391	0.008	0.579	0.020	0.141	0.305
3	0.014	0.149	0.513	0.012	0.792	0.020	0.155	0.298
5	0.020	0.113	0.608	0.025	1.008	0.023	0.138	0.401
7	0.022	0.101	0.700	0.024	1.105	0.034	0.156	0.421
10	0.031	0.147	0.871	0.033	1.209	0.050	0.193	0.476
IV	1.563	2.089	1.818	1.491	2.460	1.411	1.889	2.978
Panel C: Explained percentage variation								
1	0.969	0.703	0.931	0.970	0.981	0.977	0.966	0.902
2	0.991	0.737	0.972	0.971	0.968	0.977	0.973	0.920
3	0.979	0.770	0.948	0.934	0.926	0.983	0.966	0.936
5	0.967	0.863	0.895	0.811	0.850	0.976	0.952	0.878
7	0.961	0.883	0.866	0.747	0.819	0.949	0.931	0.846
10	0.933	0.639	0.822	0.588	0.793	0.888	0.892	0.784
IV	0.963	0.968	0.967	0.932	0.973	0.966	0.947	0.862

Entries report the mean pricing error (panel A), mean absolute pricing error (panel B), and explained variation (panel C) on CDS spreads and option implied volatilities. The pricing errors are defined as the difference between the observed CDS spreads and implied volatilities, both in percentage points, and their model-implied values. The explained variation is defined as one minus the ratio of the variance of the pricing error to the variance of the original series. The statistics on the credit default swap spreads are at each of the six fixed terms, and the statistics on the implied volatilities is on one pooled series across all maturities and strikes for each company.

specification, a highly negative skew at long option maturities can be generated from a high default arrival rate; yet, the positive mean pricing errors on the CDS spreads on these two companies suggest that the estimated default arrival rates are not high enough to match the observed CDS spreads. Taken together, the CDS and the options markets for the two companies show a degree of pricing tension within our modeling framework: The CDS spreads imply higher default arrival rates than those revealed from the option implied volatility skews.

Panel B of Table 5 reports the mean absolute pricing errors. The mean absolute pricing errors on the CDS spreads are below five basis points for the high-rating

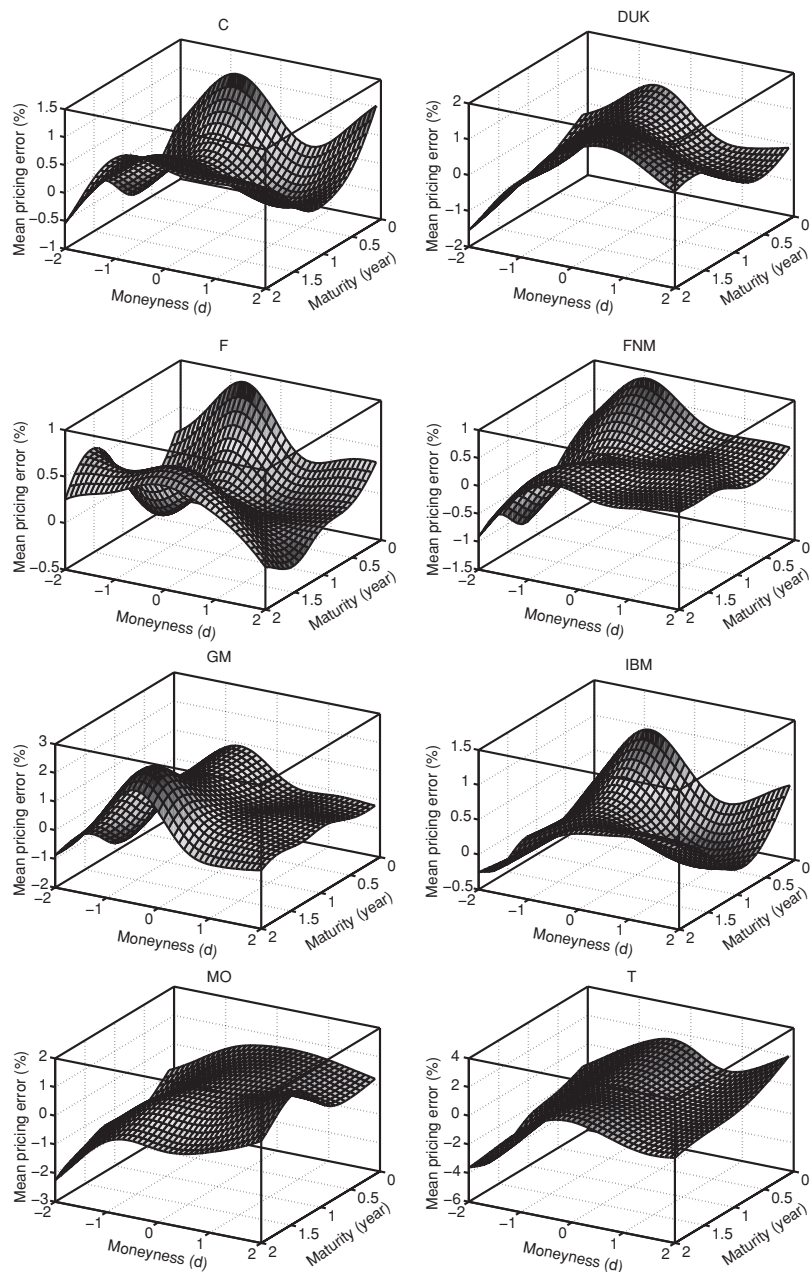


**Figure 4** Mean pricing error in implied volatility across moneyness and time to maturity. The pricing error is defined as the difference between the observed implied volatility and the corresponding model values in volatility percentage points. The mean pricing error as a function of time to maturity  $\tau$  and a standardized moneyness measure  $d$  is estimated nonparametrically with an independent bivariate Gaussian kernel. Each panel represents one company.

(A and above) and hence low-spread companies such as Citigroup, Fannie Mae, and IBM. They become larger for the low-rating/high-spread companies, 10–20 basis points for BBB-rated Duke Energy and Altria, 30–50 basis points for AT&T, 40–87 basis points for BB-rated Ford Motor, and 42–120 basis points for B-rated General Motors.

The mean absolute pricing errors on the option implied volatilities are one to three volatility points, about the same size as the average of bid-ask spreads. Figure 5 plots the nonparametrically smoothed implied volatility mean absolute pricing error surface as a function of moneyness and maturity. Overall, the mean absolute errors are larger for out-of-the-money options than for the more actively traded at-the-money options, partly as a result of our vega weighting scheme in the model estimation.

The last panel of Table 5 reports the explained variation, defined as one minus the variance ratio of the pricing errors and the original time series. The model can explain over 90% of the variation for more than half of the CDS spread series. The explained variation on the option implied volatilities are over 90% for seven of the eight companies, with the only exception being AT&T at 86%. Overall, the model generates good performance, especially when we consider the fact that we only allow two state variables ( $v_t, z_t$ ) to vary each day to capture the variations in six CDS spread series and 25–59 option prices.

## 4.2 The Joint Dynamics of Return Variance and Default Arrival Rates

Table 6 reports the maximum likelihood estimates and the absolute magnitudes of the  $t$ -statistics of the structural parameters that control the joint dynamics of the stock return variance rate and the default arrival rate. Given the large amount of data used in the model estimation, the estimates for most parameters generate large  $t$ -values and hence strong statistical significance. As the eight companies differ in credit ratings and in industry sectors, the estimated return variance and default rate dynamics also show large cross-sectional differences. Nevertheless, several common features emerge from the parameter estimates.

First, the estimates for the risk-neutral mean-reverting coefficients ( $\kappa_v, \kappa_z$ ) and their statistical counterparts ( $\kappa_v^{\mathbb{P}}, \kappa_z^{\mathbb{P}}$ ) show that the default arrival rate is more persistent than the return variance rate under both the risk-neutral measure  $\mathbb{Q}$  and the statistical measure  $\mathbb{P}$ . The difference in statistical persistence suggests that the stock return variance rates are more mean-reverting than the credit risk factor. Thus, it is more difficult to predict changes in the credit risk factor than to predict changes in the return variance rate based on their past values. The difference in risk-neutral persistence dictates that the two factors have different impacts across the term structure of options and CDS spreads. Shocks to the variance rate affect the short-term options and CDS spreads, but dissipate quickly as the option and CDS maturity increases. Shocks to the more persistent credit risk factor last longer across the term structure of options and credit spreads. In particular, the estimates for  $\kappa_z$  are not significantly different from zero for all eight companies, suggesting



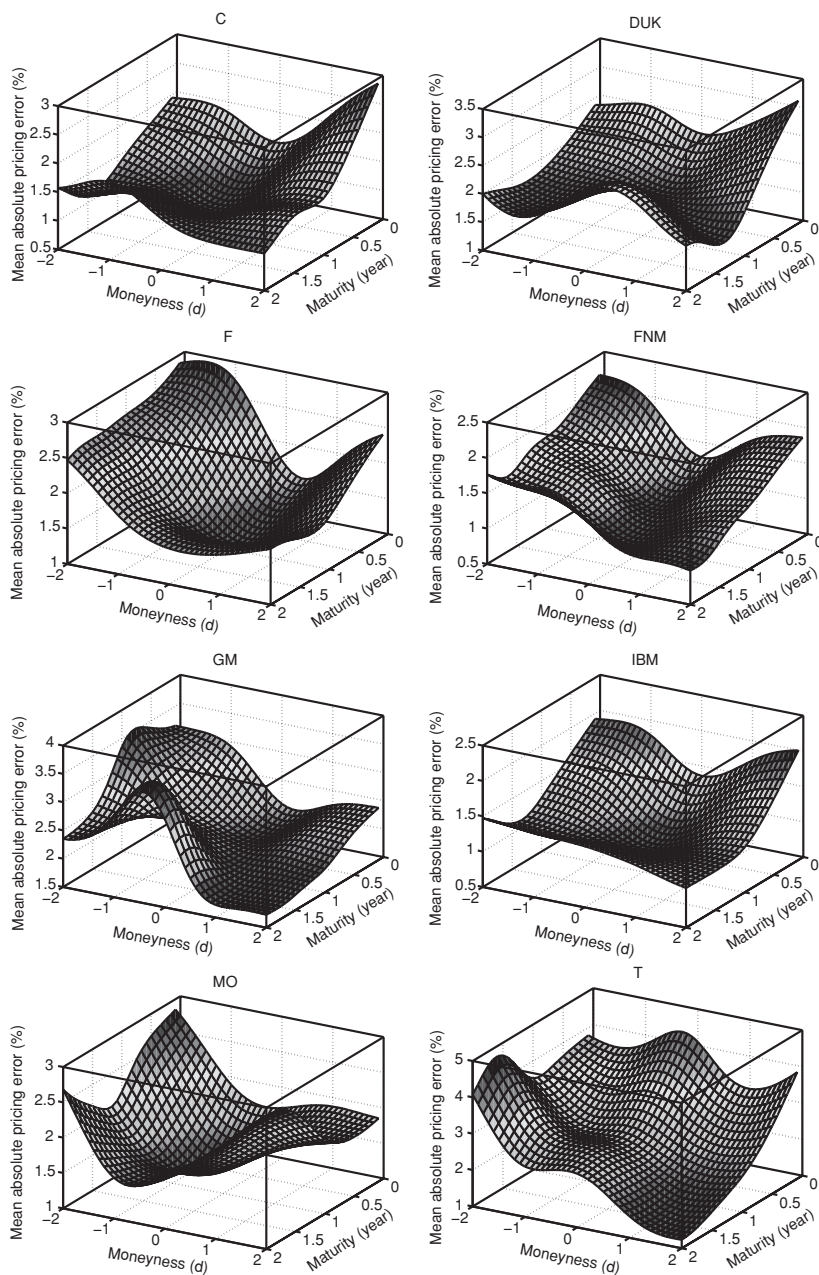


**Figure 5** Mean absolute pricing error in implied volatility across moneyiness and time to maturity. The pricing error is defined as the difference between the observed implied volatility and the corresponding model values in volatility percentage points. The mean absolute pricing error as a function of time to maturity  $\tau$  and a standardized moneyiness measure  $d$  is estimated nonparametrically with an independent bivariate Gaussian kernel. Each panel represents one company.

**Table 6** Maximum likelihood estimates of model parameters.

$\Theta$	C		DUK		F		FNM		GM		IBM		MO		T	
$\kappa_v$	0.868	(135.4)	3.092	(92.1)	0.893	(44.7)	1.476	(65.1)	1.353	(76.6)	0.802	(156.2)	2.868	(123.7)	1.089	(42.7)
$\kappa_z$	0.000	(0.0)	0.000	(0.0)	0.000	(0.0)	0.000	(0.0)	0.000	(0.0)	0.000	(0.0)	0.059	(11.8)	0.000	(0.0)
$\kappa_v^{\mathbb{P}}$	0.565	(2.6)	1.892	(4.7)	0.494	(0.9)	1.656	(2.6)	1.792	(3.2)	0.360	(1.0)	1.696	(3.9)	0.336	(0.9)
$\kappa_z^{\mathbb{P}}$	0.325	(0.5)	0.612	(0.5)	0.590	(1.0)	0.404	(0.7)	0.480	(1.2)	0.202	(0.5)	0.451	(0.5)	0.059	(0.0)
$\theta_v$	0.040	(103.6)	0.053	(8.7)	0.048	(22.2)	0.072	(58.9)	0.071	(17.8)	0.026	(64.4)	0.105	(52.5)	0.018	(3.7)
$\theta_z$	0.001	(130.9)	0.006	(15.3)	0.008	(30.3)	0.001	(6.5)	0.009	(57.7)	0.002	(71.0)	0.004	(64.7)	0.003	(33.2)
$\sigma_v$	0.281	(33.8)	0.267	(13.8)	0.332	(35.4)	0.387	(38.6)	0.497	(29.1)	0.200	(36.6)	0.398	(41.9)	0.137	(7.3)
$\sigma_z$	0.036	(12.6)	0.315	(23.0)	0.187	(19.0)	0.027	(9.9)	0.250	(39.4)	0.069	(19.6)	0.245	(42.3)	0.204	(14.2)
$\beta$	0.000	(0.0)	0.000	(0.0)	0.004	(0.3)	0.000	(0.0)	0.000	(0.0)	0.000	(0.0)	0.001	(0.2)	0.000	(0.0)
$\rho$	-0.558	(58.4)	-0.206	(6.5)	-0.423	(17.0)	-0.720	(54.5)	-0.832	(27.0)	-0.518	(35.9)	-0.572	(30.9)	-0.379	(5.4)
$\zeta$	3.818	(21.8)	69.176	(4.0)	3.406	(5.2)	9.515	(12.7)	24.070	(4.1)	13.995	(13.7)	13.216	(11.8)	973.654	(1.3)
$v_+$	0.000	(0.0)	0.064	(16.7)	0.204	(22.9)	0.110	(41.6)	0.099	(17.9)	0.077	(31.6)	0.118	(48.4)	0.000	(0.0)
$v_-$	0.461	(49.6)	0.169	(17.7)	0.475	(11.3)	0.290	(32.7)	0.151	(12.9)	0.202	(37.2)	0.214	(32.7)	0.043	(5.8)
$w$	0.000	(0.0)	0.672	(257.0)	0.001	(0.1)	0.002	(0.0)	0.000	(0.0)	0.657	(182.7)	0.001	(0.4)	0.000	(0.0)
$\sigma_C^2$	0.012	(43.6)	0.116	(109.6)	0.030	(32.7)	0.013	(23.0)	0.032	(84.6)	0.012	(36.8)	0.008	(51.2)	0.038	(58.5)
$\sigma_O^2$	0.045	(193.5)	0.083	(122.8)	0.067	(99.8)	0.042	(183.0)	0.138	(269.9)	0.035	(335.3)	0.054	(231.7)	0.204	(254.6)
$\gamma_v$	1.076	(1.4)	4.493	(2.7)	1.200	(0.7)	-0.465	(0.3)	-0.883	(0.8)	2.200	(1.2)	2.947	(2.5)	5.490	(1.9)
$\gamma_z$	-9.071	(0.5)	-1.943	(0.5)	-3.161	(1.1)	-15.087	(0.7)	-1.917	(1.2)	-2.920	(0.5)	-1.597	(0.4)	-0.291	(0.0)

Absolute magnitudes of the  $t$ -statistics are given in parentheses. The estimation is based on weekly sampled data from May 8, 2002 to May 10, 2006.

that a shock to the credit risk factor generates relatively uniform responses from credit spreads of all maturities. As such, long-term CDS spreads vary as much as short-term CDS spreads.

For each risk factor, the difference in persistence under the two probability measures defines the market price of that factor's risk:

$$\gamma_v = \kappa_v - \kappa_v^{\mathbb{P}} / \sigma_v, \quad \gamma_z = \kappa_z - \kappa_z^{\mathbb{P}} / \sigma_z. \quad (27)$$

We compute the market price of risk coefficients ( $\gamma_v, \gamma_z$ ) based on the parameter estimates and report them in the last two rows of Table 6. The estimates for the market price of variance rate risk ( $\gamma_v$ ) are mostly positive or insignificantly different from zero. By contrast, the estimates for the market price of the default arrival rate risk ( $\gamma_z$ ) are negative for all eight companies.

Several studies, for example, Bakshi and Kapadia (2003a, 2003b) and Carr and Wu (2009), use stock and stock index options and the underlying time series returns to study the total return variance risk premia. They find that the risk premia are negative for some stocks, and highly negative for stock indexes. Our model decomposes the total risk on an individual stock into two components: risk in the return variance rate under normal market conditions and risk in the default arrival rate. By using both the CDS data and stock options data, we are able to separate the two sources of risks and identify their respective market prices. Our estimation suggests that for the eight stocks, negative risk premia only come from the default arrival rate, but not from the return variance rate.

Another common finding among the eight reference companies is that the estimated loading ( $\beta$ ) of the return variance rate on the default arrival rate is close to zero. Even though there is evidence that companies with high credit spreads also tend to have high equity return volatility levels on average (e.g., Campbell and Taksler, 2003), our near-zero estimates on the loading coefficient suggest that the two derivatives markets (CDS spreads and stock options) contain a large proportion of independent instantaneous variations that we must capture through the separate variations of the two risk factors  $v_t$  and  $z_t$ . When  $\beta = 0$ , the CDS spreads become independent of the return variance rate  $v_t$  and are fully determined by the credit risk factor  $\lambda_t = z_t$ . Nevertheless, the option implied volatilities are still a function of the credit risk factor  $z_t$  as the default arrival rate directly enters the valuation of the stock options. The observed correlations between CDS spreads and the option implied volatilities are driven purely by their common loading on the credit risk factor.

For all eight companies, the estimates for the instantaneous correlation between stock return and return variance  $\rho$  are negative, consistent with the classic leverage effect explanation. Nevertheless, by allowing the possibility of default to contribute to the negative option implied volatility skew, the negative correlation estimates are low compared to some estimates in the literature.

In addition to the rare but catastrophic event of default, we also allow the stock price to move discontinuously under normal market conditions. We capture this discontinuous movements using a high-frequency variance-gamma jump

component, with  $v_+$  and  $v_-$  capturing the relative jump size differences for upside and downside jumps under the risk-neutral measure. For all eight companies, the estimates for the upside jump sizes are much smaller than are the estimates for the downside jump sizes. The estimated jump size asymmetry contributes to the negative option implied volatility skew at short maturities.

Finally, the literature often finds it difficult to separately identify the recovery rate and the default arrival rate using credit spread data alone (Houweling and Vorst, 2005; Hull and White, 2000; Longstaff, Mithal, and Neis, 2005). As a result, researchers often assume a fixed recovery rate instead of estimating it along with other model parameters. By exploiting the overlapping information from the stock options market and the CDS market, we are able to separately identify the recovery rate  $w$  and the default arrival rate dynamics. The recovery rate estimates vary greatly across different companies, from virtually zero recovery to as high as 67%.

Several caveats apply to the interpretation of the parameter estimates. First, we assume that the stock price drops to zero upon default. The bond recovery identification hinges on the zero recovery assumption on equity. Second, the joint estimation relies on the assumption that the two markets are integrated and that the same risk is priced identically in the two markets. When the two markets are segmented and the prices from the two markets are not completely consistent with each other, the tension can show up both in the parameter estimates and the pricing errors. For example, for companies such as Altria and AT&T, the mean pricing errors on the implied volatility surface (Figure 4) and the CDS spreads (Table 5) suggest that the CDS spreads are too wide relative to the steepness of the implied volatility skews. With this tension between the two markets, fitting the relatively flat implied volatility skew generates a small estimate on the default arrival rate  $\lambda_t$ . To fit the relatively wide CDS spreads at the same time, the estimation can only choose a low bond recovery rate. The opposite would be the case if the options are priced more expensively than the CDS spreads. Thus, the recovery rate estimates can be affected by the tensions between the two markets. Finally, when market segmentation generates large idiosyncratic noise in the two markets, the noise will reduce the observed co-movements between the CDS spreads and the implied volatilities, and accordingly lower the estimated loading ( $\beta$ ) of the return variance rate on the default arrival rate.

### 4.3 The Term Structure of Credit Default Swap Spreads

Given the model parameter estimates in Table 6, we can compute the term structures of the CDS spreads at different levels of the credit risk factor  $z$ . In Figure 6, we plot the model-implied mean term structure of the CDS spreads in solid lines, where we set the risk levels to their respective sample averages. The two dashed lines in each panel are constructed by setting the variance rate  $v$  to its sample mean and the credit risk factor  $z_t$  to its 10th and 90th percentile values. Since the loading estimates ( $\beta$ ) of the return variance rate  $v_t$  to the default arrival rate are close to zero for all eight companies, shocks on the return variance rate have negligible impacts

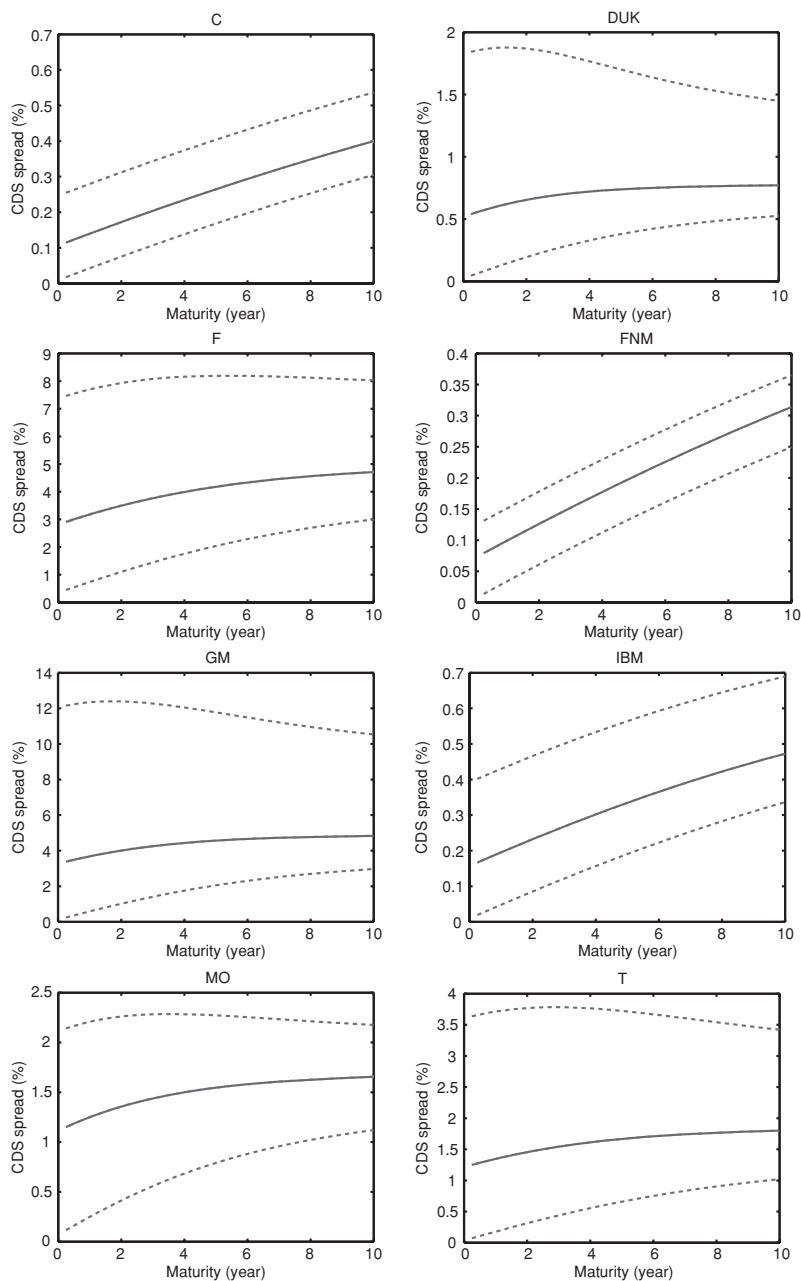


**Figure 6** The term structure of credit default swap spreads. The solid lines represent the mean term structures computed from the estimated model and the sample mean levels of the two risk factors. The two dashed lines in each panel are computed by setting the return variance rate  $v_t$  to the sample average and  $z_t$  to its 10th and 90th percentile values.

on the CDS spreads. Thus, we focus the analysis on the impact of the credit risk factor on the CDS term structure.

The estimated model parameters on the eight companies generate different average term structure shapes on the CDS spreads. Nevertheless, the impacts of the credit risk factor show similar patterns. Given the high risk-neutral persistence on the credit risk factor, shocks to this factor generate similar responses from CDS spreads at both short and long maturities. A shift in the credit risk factor  $z_t$  leads to nearly parallel shifts in the CDS term structure.

#### 4.4 The Implied Volatility Skew and Term Structure

To understand how the two risk factors contribute to the pricing of stock options, we compute and plot the one-month implied volatility skew across different moneyness levels in Figure 7 at different risk levels. In computing the option values and constructing the implied volatility skews as a function of moneyness, we assume zero interest rates and dividend yields, and define the moneyness as  $\ln(K/S)/\sqrt{v\tau}$ . The solid lines are the mean implied volatility skews evaluated at the sample means of the two risk factors. The two dashed lines in each panel are generated with the variance rate fixed at its sample mean and the credit risk factor at its 10th and 90th percentile values. Hence, they capture the impact of shocks from the credit risk factor. The two dash-dotted lines in each panel are generated by fixing the credit risk factor at its sample mean and setting the variance rate at its 10th and 90th percentile values. Hence, the dotted lines capture the impact of shocks from the return variance rate.

For all eight companies, the mean implied volatilities show similar skewed patterns across moneyness. Variations in the variance rate level lead to relatively uniform (parallel) shifts in the implied volatility skew across moneyness. In contrast, the impact of the credit risk factor is mainly at low strikes. The impact of the credit risk factor on far out-of-the-money call option implied volatilities at high strikes is small. Since the main effect of default on equity is to drive the stock price to zero, it is understandable that the credit risk factor has its major impacts on far out-of-the-money put options.

To see how the effects change at different maturities, we also plot in Figure 8 the corresponding implied volatility skew for one-year options. Similar to the effects on the one-month implied volatility skew, the shocks on the variance rate generate relatively uniform responses across moneyness (dash-dotted lines), whereas shocks on the credit risk factor generate larger impacts at lower strikes (dashed lines). Comparing Figures 7 and 8 also brings out visible differences: The impact of the credit risk factor becomes much larger at longer maturities. The exceptions are on the AAA-rated Fannie Mae and AA-rated Citigroup, for which the default probabilities are so small that their impacts on the implied volatilities are minimal across all maturities.

Figure 9 plots the term structure of the at-the-money implied volatilities at different risk levels. Again, we use the solid lines to denote the mean term structure, the dashed lines to capture the impact of credit risk shocks, and the dash-dotted

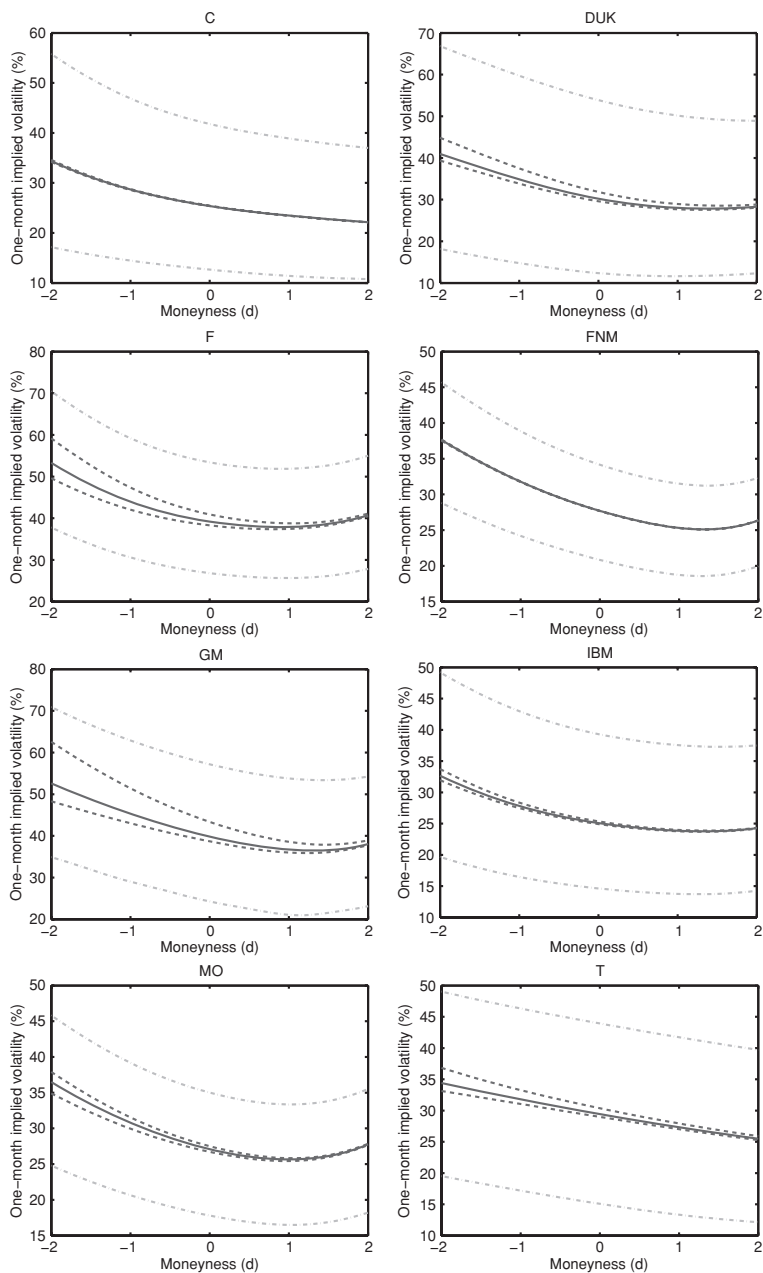


**Figure 7** The one-month implied volatility smirks. The solid lines are the mean implied volatility across moneyiness at one-month maturity computed from the estimated model and the sample mean levels of the two risk factors. Moneyiness is defined as  $d = \ln(K/S)/\sqrt{v\tau}$ . Dashed lines are computed by setting  $v_t$  to its sample average and  $z_t$  to its 10th and 90th percentile values. Dash-dotted lines are computed by setting  $z_t$  to the sample mean and  $v_t$  to its 10th and 90th percentile values.

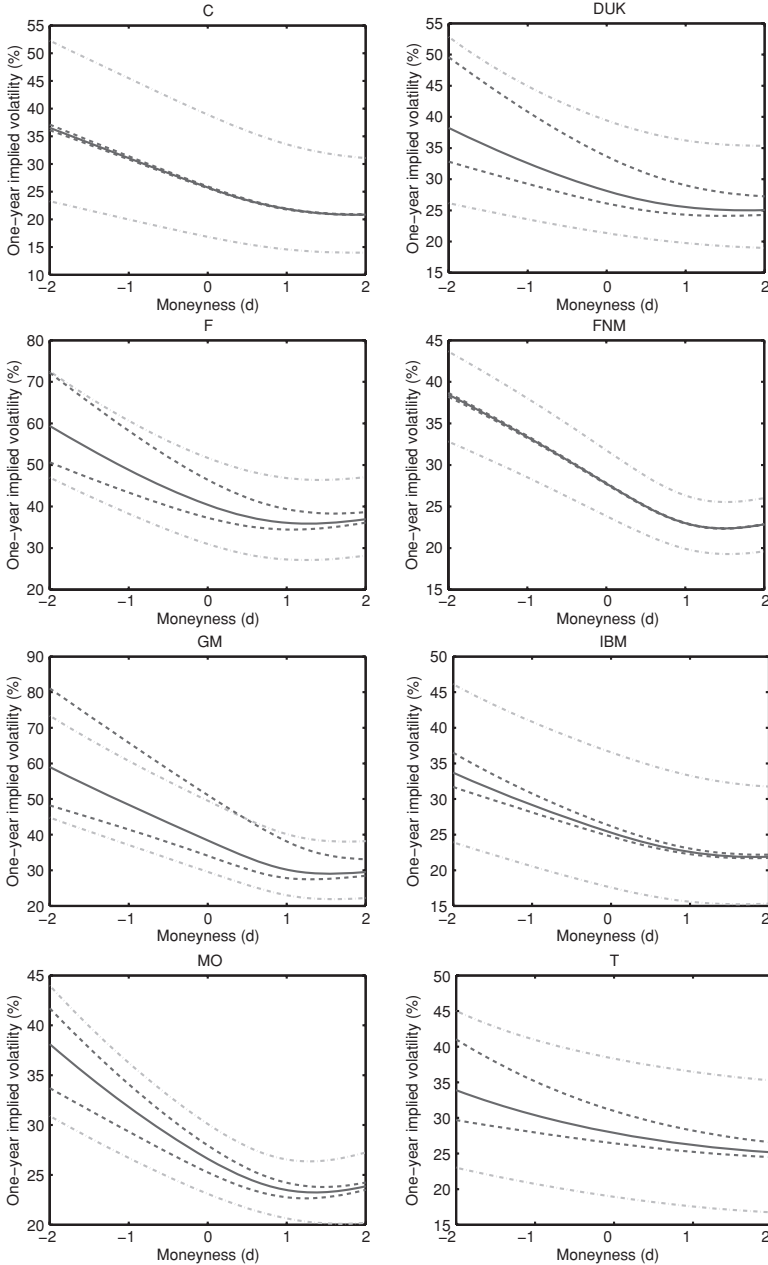


**Figure 8** The one-year implied volatility skews. The solid lines are the mean implied volatility across moneyiness at one-year maturity computed from the estimated model and the sample mean levels of the two risk factors. Moneyiness is defined as  $d = \ln(K/S)/\sqrt{v\tau}$ . Dashed lines are computed by setting  $v_t$  to its sample average and  $z_t$  to its 10th and 90th percentile values. Dash-dotted lines are computed by setting  $z_t$  to the sample mean and  $v_t$  to its 10th and 90th percentile values.



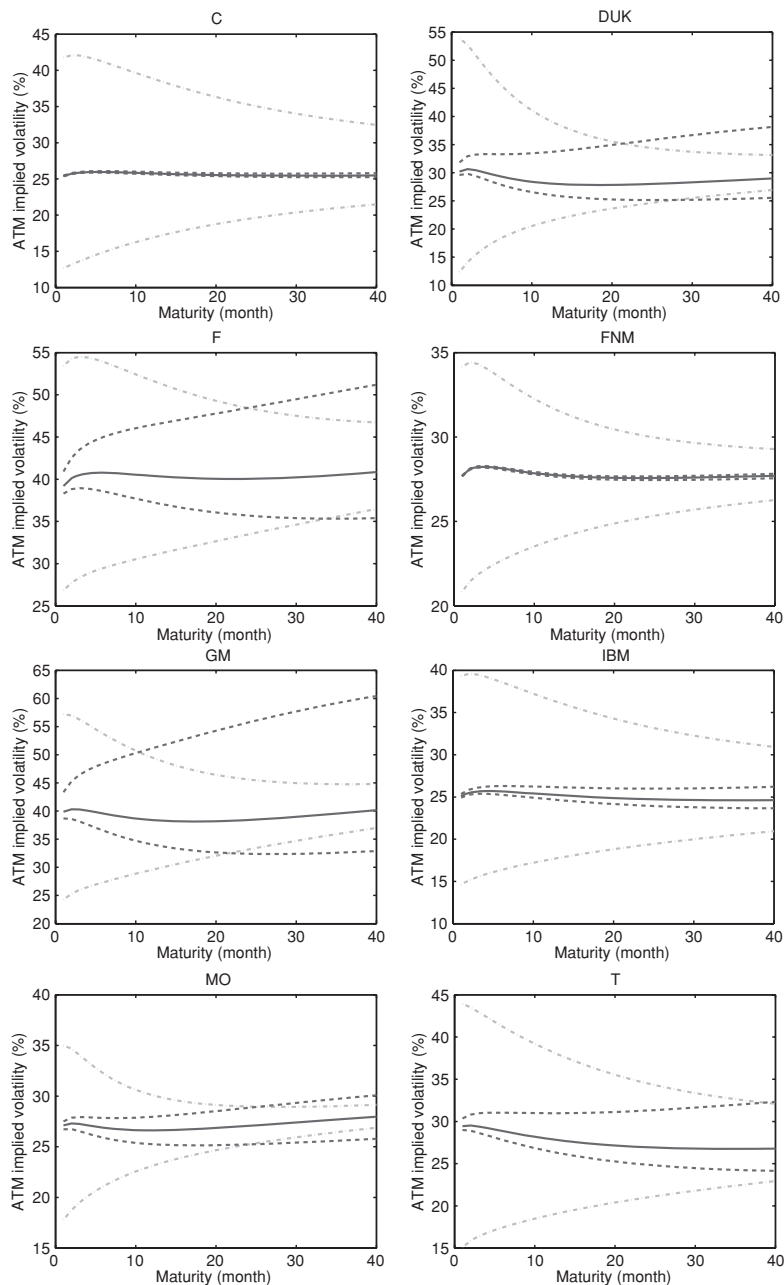


**Figure 9** The term structure of at-the-money implied volatilities. The solid lines are the mean term structure of the at-the-money implied volatility computed from the estimated model and at the sample mean levels of the two risk factors. Dashed lines are computed by setting  $v_t$  to its sample average and  $z_t$  to its 10th and 90th percentile values. Dash-dotted lines are computed by setting  $z_t$  to the sample mean and  $v_t$  to its 10th and 90th percentile values.

lines to capture the impact of the return variance rate shocks. At short option maturities, the impact of the return variance rate is much larger than the impact of the credit risk factor. However, as maturity increases, the influence of the return variance rate declines due to its mean-reverting behavior. By contrast, the influence of the credit risk factor increases due to its high risk-neutral persistence, especially for low-rating companies. For companies with BBB or lower credit ratings, the default risk contributes to the option implied volatility as much as the return variance risk does when the option maturity is two years or longer.

## 5 SUMMARY AND CONCLUSIONS

Based on documented evidence on the joint movements between CDS spreads and stock option implied volatilities and implied volatility skews, we propose a dynamically consistent framework for the joint valuation and estimation of stock options and CDS spreads written on the same reference company. We model the possible default of a company by a Cox process with a stochastic arrival rate, and we assume that the stock price falls to zero upon default. We model the pre-default stock price as following a jump-diffusion process with stochastic volatility. We assume that the default arrival rate and the return variance rate follow a bivariate diffusion with dynamic interactions that match the empirical evidence linking stock option implied volatilities and CDS spreads. Importantly, our dynamic specification allows both common movements and independent variations between the two markets.

Under this joint specification, we derive tractable pricing solutions for stock options and credit default swaps. We estimate the joint dynamics of the variance rate and the default arrival rate using data on stock option implied volatilities and CDS spreads for eight companies that span a wide spectrum of industry sectors and credit rating classes. Estimation results show that the default arrival rate is much more persistent than the variance rate under both the statistical measure and the risk-neutral measure. The statistical persistence difference suggests different degrees of predictability. The risk-neutral difference in persistence suggests that the default arrival rate has a more long-lasting impact on the term structure of option volatilities and CDS spreads than does the return variance.

The estimation also highlights the interaction between market and credit risk in pricing stock options and credit default swaps. The default arrival rate affects stock option pricing through its direct effect on the risk-neutral drift of the return process. We find that the impact of the diffusion variance rate on the implied volatility is relatively uniform across different moneyness levels, while the impact of the credit risk factor is mainly on options at low strikes. Furthermore, the impact of the credit risk factor on stock options prices increases with the option maturity. At long option maturities and for companies with significant default risks, the contribution of the credit risk factor to option pricing can be as large as the contribution of the return variance rate. We conclude that one can learn more about stock options and CDS by developing a model that integrates both markets, rather than having separate models for each market.

## APPENDIX

### A Generalized Fourier Transform of Stock Returns

To derive the generalized Fourier transform

$$\phi(u) \equiv \mathbb{E}_t \exp \left[ - \int_t^T \lambda_s ds \right] e^{iu \ln P_T/P_t}, \quad u \in \mathcal{D} \subset \mathbb{C}, \quad (\text{A1})$$

we use the language of stochastic time change of Carr and Wu (2004) and define

$$T_t \equiv \int_t^T v_s ds, \quad T_t^z \equiv \int_t^T z_s ds, \quad T_t^\lambda \equiv \int_t^T \lambda_s ds = T_t^z + \beta T_t.$$

Then, conditional on no default during the time horizon  $[t, T]$ , with  $\tau = T - t$ , we can write the log stock return as

$$\ln(P_T/P_t) = (r(t, T) - q(t, T))\tau + T_t^\lambda + (W^P + J^P)_{T_t} - \frac{1}{2} + k_J(1) T_t, \quad (\text{A2})$$

where  $r(t, T)$  and  $q(t, T)$  denote the continuously compounded spot interest rates and dividend yields of the relevant maturity;  $J_t^P$  denotes a pure-jump Lévy process with the jump arrival rate controlled by the Lévy density  $\pi(x)$  specified in (2); and  $k_J(s)$  denotes the cumulant exponent of the Lévy jump,

$$k_J(s) \equiv \ln \mathbb{E} e^{sJ_t^P} = -\zeta \ln(1 - sv_+)(1 + sv_-). \quad (\text{A3})$$

The discounted generalized Fourier transform becomes

$$\begin{aligned} \phi(u) &= \mathbb{E}_t \exp \left( - T_t^\lambda + iu(r(t, T) - q(t, T))\tau + iuT_t^\lambda + iu(W^P + J^P)_{T_t} \right. \\ &\quad \left. - \frac{1}{2} + k_J(1) iuT_t \right) = \exp(iu(r(t, T) - q(t, T))\tau) \mathbb{E}_t^{\mathbb{M}} \exp \left( - (1 - iu)T_t^\lambda \right. \\ &\quad \left. - \frac{1}{2}(iu + u^2) + \psi_J(u) T_t \right) = \exp(iu(r(t, T) - q(t, T))\tau) \mathbb{E}_t^{\mathbb{M}} \\ &\quad \times \exp \left( -(1 - iu)T_t^z - (1 - iu)\beta + \frac{1}{2}(iu + u^2) + \psi_J(u) T_t \right), \quad (\text{A4}) \end{aligned}$$

where the new measure  $\mathbb{M}$  is defined by the following complex-valued exponential martingale:

$$\frac{d\mathbb{M}}{d\mathbb{Q}} \Big|_t = \exp \left( iu(W^P + J^P)_{T_t} + \frac{1}{2}u^2 + \zeta \ln(1 - iuv_+)(1 + iuv_-) T_t \right);$$

and  $\psi_J(u) = \zeta(\ln(1 - iuv_+)(1 + iuv_-) - iu \ln(1 - v_+)(1 + v_-))$  is the characteristic exponent of the convexity-adjusted jump component.

Under the new measure  $\mathbb{M}$ , the drift of the variance rate dynamics changes to  $\mu_v^{\mathbb{M}} = \theta_v - \kappa_v^{\mathbb{M}} v(t)$ , with  $\kappa_v^{\mathbb{M}} = \kappa_v - iu\sigma_v\rho$ . The dynamics of  $z_t$  does not change as its variation is independent of the stock return innovations  $W^P$  and  $J^P$ . We can rewrite the expectation in the last line of Equation (A4) as

$$\phi(u) = \exp(iu(r(t, T) - q(t, T))\tau) \mathbb{E}_t^{\mathbb{M}} \exp - \int_t^T b_0^\top x_s ds$$

with  $x_t = [v_t, z_t]^\top$ ,  $b_0 = [b_v, b_z]^\top$ ,  $b_v = (1 - iu)\beta + \frac{1}{2}(iu + u^2) + \psi_f(u)$ , and  $b_z = 1 - iu$ . Since the risk factors  $x$  follow affine dynamics, the solution to the expectation is exponential affine in  $x_t$ ,

$$\phi(u) = \exp(iu(r(t, T) - q(t, T))\tau) \exp(-a(\tau) - b(\tau)^\top x_t),$$

where the coefficients can be solved analytically as in (11) and (12).

## B Unscented Kalman Filter and Maximum Likelihood Estimation

To estimate the model parameters, we cast the model into a state-space form, which consists of a set of state propagation equations as in Equation (24) and measurement equations as in Equation (25). We rewrite them in canonical forms:

$$x_t = A + \Phi x_{t-1} + \overline{Q_{t-1}} \varepsilon_t, \quad \varepsilon_t \sim N(0, I), \quad (\text{B1})$$

$$y_t = h(x_t) + e_t, \quad e_t \sim N(0, R). \quad (\text{B2})$$

Let  $\bar{x}_t$ ,  $\bar{\Sigma}_{xx,t}$ ,  $\bar{y}_t$ ,  $\bar{\Sigma}_{yy,t}$  denote the time- $(t-1)$  forecasts of time- $t$  values of the state vector, the covariance of the state vector, the measurement series, and the covariance of the measurement series. Let  $\hat{x}_t$  and  $\hat{\Sigma}_{xx,t}$  denote the *ex post* updates on the state vector and its covariance at the time  $t$  based on observations ( $y_t$ ) at time  $t$ . In the case of linear measurement equations,

$$y_t = Hx_t + e_t, \quad (\text{B3})$$

the Kalman filter generates efficient forecasts and updates on the conditional mean and covariance of the state vector and the measurement series. The Kalman filter predictions on the state vector are

$$\bar{x}_t = A + \Phi \hat{x}_{t-1}, \quad \bar{\Sigma}_{xx,t} = \Phi \hat{\Sigma}_{xx,t-1} \Phi^\top + Q_{t-1}. \quad (\text{B4})$$

The predictions on the measurement and its variance and covariance with the state are

$$\bar{y}_t = H\bar{x}_t, \quad \bar{\Sigma}_{yy,t} = H\bar{\Sigma}_{xx,t}H^\top + R, \quad \bar{\Sigma}_{xy,t} = \bar{\Sigma}_{xy,t}H^\top. \quad (\text{B5})$$

With new observations  $y_t$ , the updated mean and covariance of the state vector become

$$\hat{x}_t = \bar{x}_t + K_t(y_t - \bar{y}_t), \quad \hat{\Sigma}_{xx,t} = \bar{\Sigma}_{xx,t} - K_t\bar{\Sigma}_{yy,t}K_t^\top, \quad (\text{B6})$$

where  $K_t = \bar{\Sigma}_{xy,t}(\bar{\Sigma}_{yy,t})^{-1}$  is the Kalman gain.

In our application, the state propagation in (B1) remains Gaussian linear, but the measurement equation in (B2) is nonlinear. We take the unscented Kalman filter approach and use a set of deterministically chosen sigma points to approximate the distribution of the state vector. We perform the nonlinear measurement transformation on these sigma points and compute the mean and covariances of measurements from these transformed points.

Specifically, let  $p$  be the number of states,  $\delta > 0$  be a control parameter, and  $\chi_i$  be the  $i$ th column of a matrix  $\chi$ , we can generate a set of  $2p + 1$  sigma vectors  $\chi_i$  based on the mean and covariance estimates on the state vector. Taking the time- $t$  forecasted mean and covariance ( $\bar{x}_t$  and  $\overline{xx}_t$ ) as an example, we have

$$\chi_{t,0} = \bar{x}_t, \quad \chi_{t,i} = \bar{x}_t \pm \sqrt{(p + \delta)(\overline{xx}_t)}_j, \quad j = 1, \dots, p; \quad i = 1, \dots, 2p \quad (\text{B7})$$

with corresponding weights  $w_i$  given by

$$w_0 = \delta / (p + \delta), \quad w_i = 1 / [2(p + \delta)], \quad j = 1, \dots, 2p. \quad (\text{B8})$$

We can regard these sigma vectors as forming a discrete distribution with  $w_i$  being the corresponding probabilities. We can verify that the mean and covariance of this distribution are  $\bar{x}_t$  and  $\overline{xx}_t$ , respectively.

Given the Gaussian-linear structure of the state propagation equation, we can still use Equation (B5) to predict the mean and covariance of the state vector  $\bar{x}_t$  and  $\overline{xx}_t$ . Then, we generate the sigma points based on the predicted mean and covariance according to Equations (B7) and (B8), and use these sigma points to predict the mean and covariances of the measurement series:

$$\begin{aligned} \bar{y}_t &= \sum_{i=0}^{2p} w_i h(\chi_{t,i}; \Theta), \\ \overline{yy}_t &= \sum_{i=0}^{2p} w_i [h(\chi_{t,i}; \Theta) - \bar{y}_t][h(\chi_{t,i}; \Theta) - \bar{y}_t]^\top + R, \\ \overline{xy}_t &= \sum_{i=0}^{2p} w_i [\chi_{t,i} - \bar{x}_t][h(\chi_{t,i}; \Theta) - \bar{y}_t]^\top. \end{aligned} \quad (\text{B9})$$

With these predicted moments, the filtering follows the same steps as in Equation (B6).

We define the log-likelihood for each day's observations assuming that the forecasting errors are normally distributed:

$$l_t(\Theta) = -\frac{1}{2} \log |\overline{yy}_t| - \frac{1}{2} (y_t - \bar{y}_t)^\top (\overline{yy}_t)^{-1} (y_t - \bar{y}_t). \quad (\text{B10})$$

To attach equal weights to the CDS and the options markets, we partition the observations from the two markets and define the log-likelihood for each market separately,  $l_t^C(\Theta)$  for the CDS market and  $l_t^O(\Theta)$  for the options market. We scale the two log-likelihood values by the corresponding number of observations each day before we perform the maximization on the sum of the log-likelihood values to obtain the model parameters

$$\Theta \equiv \arg \max_{\Theta} \sum_{t=1}^N l_t^C(\Theta) / n_t^C + l_t^O(\Theta) / n_t^O, \quad (\text{B11})$$

where  $N = 210$  denotes number of days in our sample and  $n_t^C$  and  $n_t^O$  denote the number of CDS and option observations each day. We have six CDS series ( $n_t^C = 6$  for all  $t$ ) at six fixed time to maturities. The number of option observations  $n_t^O$  varies across different reference companies and different days.

*Received January 22, 2009; revised May 8, 2009; accepted June 1, 2009.*

## REFERENCES

- Acharya, V. V., and J. Carpenter. 2002. Corporate Bond Valuation and Hedging with Stochastic Interest Rates and Endogenous Bankruptcy. *Review of Financial Studies* 15: 1355–1383.
- Anderson, R. W., and S. Sundaresan. 1996. Design and Valuation of Debt Contracts. *Review of Financial Studies* 9: 37–68.
- Anderson, R. W., S. Sundaresan, and P. Tychon. 1996. Strategic Analysis of Contingent Claims. *European Economic Review* 40: 871–881.
- Bakshi, G., and N. Kapadia. 2003a. Delta-Hedged Gains and the Negative Market Volatility Risk Premium. *Review of Financial Studies* 16: 527–566.
- Bakshi, G., and N. Kapadia. 2003b. Volatility Risk Premium Embedded in Individual Equity Options: Some New Insights. *Journal of Derivatives* 11: 45–54.
- Bakshi, G., N. Kapadia, and D. Madan. 2003. Stock Return Characteristics, Skew Laws, and the Differential Pricing of Individual Equity Options. *Review of Financial Studies* 16: 101–143.
- Bakshi, G., D. Madan, and F. Zhang. 2006. Investigating the Role of Systematic and Firm-Specific Factors in Default Risk: Lessons from Empirically Evaluating Credit Risk Models. *Journal of Business* 79: 1955–1987.
- Bekaert, G., and G. Wu. 2000. Asymmetric Volatilities and Risk in Equity Markets. *Review of Financial Studies* 13: 1–42.
- Bhamra, H. S., L.-A. Kuehn, and I. A. Strebulaev. 2007. “The Levered Equity Risk Premium and Credit Spreads: A Unified Framework.” Working paper, University of British Columbia and Stanford University.
- Black, F. 1976. The Pricing of Commodity Contracts. *Journal of Financial Economics* 3: 167–179.
- Black, F., and J. C. Cox. 1976. Valuing Corporate Securities: Some Effects of Bond Indenture Provisions. *Journal of Finance* 31: 351–367.
- Black, F., and M. Scholes. 1973. The Pricing of Options and Corporate Liabilities. *Journal of Political Economy* 81: 637–654.
- Briys, E., and F. de Varenne. 1997. Valuing Risky Fixed Rate Debt: An Extension. *Journal of Financial and Quantitative Analysis* 32: 239–248.
- Buraschi, A., F. Trojani, and A. Vedolin. 2007. “The Joint Behavior of Credit Spreads, Stock Options and Equity Returns When Investors Disagree.” Working paper, Imperial College and University of St. Gallen.
- Campbell, J. Y., and L. Hentschel. 1992. No News Is Good News: An Asymmetric Model of Changing Volatility in Stock Returns. *Review of Economic Studies* 31: 281–318.

- Campbell, J. Y., and A. S. Kyle. 1993. Smart Money, Noise Trading and Stock Price Behavior. *Review of Economic Studies* 60: 1–34.
- Campbell, J. Y., and G. B. Taksler. 2003. Equity Volatility and Corporate Bond Yields. *Journal of Finance* 63: 2321–2349.
- Carr, P., H. Geman, D. Madan, and M. Yor. 2002. The Fine Structure of Asset Returns: An Empirical Investigation. *Journal of Business* 75: 305–332.
- Carr, P., and V. Linetsky. 2006. A Jump to Default Extended CEV Model: An Application of Bessel Processes. *Finance and Stochastics* 10: 303–330.
- Carr, P., and L. Wu. 2003a. Finite Moment Log Stable Process and Option Pricing. *Journal of Finance* 58: 753–777.
- Carr, P., and L. Wu. 2003b. What Type of Process Underlies Options? A Simple Robust Test. *Journal of Finance* 58: 2581–2610.
- Carr, P., and L. Wu. 2004. Time-Changed Lévy Processes and Option Pricing. *Journal of Financial Economics* 71: 113–141.
- Carr, P., and L. Wu. 2008a. “Leverage Effect, Volatility Feedback, and Self-Exciting Market Disruptions: Disentangling the Multi-dimensional Variations in S&P 500 Index Options.” Working paper, Bloomberg and Baruch College.
- Carr, P., and L. Wu. 2008b. “A Simple Robust Link between American Puts and Credit Protection.” Working paper, Bloomberg and Baruch College.
- Carr, P., and L. Wu. 2009. Variance Risk Premiums. *Review of Financial Studies* 22: 1311–1341.
- Chen, L., P. Collin-Dufresne, and R. S. Goldstein. 2008. On the Relation between the Credit Spread Puzzle and the Equity Premium Puzzle. *Review of Financial Studies* (in press).
- Collin-Dufresne, P., R. S. Goldstein, and J. S. Martin. 2001. The Determinants of Credit Spread Changes. *Journal of Finance* 56: 2177–2207.
- Consigli, G. 2004. “Credit Default Swaps and Equity Volatility: Theoretical Modelling and Market Evidence.” Working paper, University Ca’Foscari.
- Cremers, M., J. Driessen, and P. J. Maenhout. 2008. Explaining the Level of Credit Spreads: Option-Implied Jump Risk Premia in a Firm Value Model. *Review of Financial Studies* (in press).
- Cremers, M., J. Driessen, P. J. Maenhout, and D. Weinbaum. 2008. Individual Stock-Option Prices and Credit Spreads. *Journal of Banking and Finance* (in press).
- Das, S. R., and R. K. Sundaram. 2004. “A Simple Model for Pricing Securities with Equity, Interest-Rate, and Default Risk.” Working paper, Santa Clara University and New York University.
- Dennis, P., and S. Mayhew. 2002. Risk-neutral Skewness: Evidence from Stock Options. *Journal of Financial and Quantitative Analysis* 37: 471–493.
- Duffie, D., and D. Lando. 2001. Term Structure of Credit Spreads with Incomplete Accounting Information. *Econometrica* 9: 633–664.
- Duffie, D., J. Pan, and K. Singleton. 2000. Transform Analysis and Asset Pricing for Affine Jump Diffusions. *Econometrica* 68: 1343–1376.
- Fan, H., and S. M. Sundaresan. 2000. Debt Valuation, Renegotiation and Optimal Dividend Policy. *Review of Financial Studies* 13: 1057–1099.
- Garbade, K. D. 1999. Managerial Discretion and the Contingent Valuation of Corporate Securities. *Journal of Derivatives* 6: 65–76.

- Geske, R. 1977. The Valuation of Corporate Liabilities as Compound Options. *Journal of Financial and Quantitative Analysis* 12: 541–552.
- Goldstein, R., N. Ju, and H. Leland. 2001. An EBIT-based Model of Dynamic Capital Structure. *Journal of Business* 74: 483–512.
- Haugen, R. A., E. Talmor, and W. N. Torous. 1991. The Effect of Volatility Changes on the Level of Stock Prices and Subsequent Expected Returns. *Journal of Finance* 46: 985–1007.
- Ho, T. S., and R. F. Singer. 1982. Bond Indenture Provisions and the Risk of Corporate Debt. *Journal of Financial Economics* 10: 375–406.
- Houweling, P., and T. Vorst. 2005. Pricing Default Swaps: Empirical Evidence. *Journal of International Money and Finance* 24: 1200–1225.
- Huang, J., and L. Wu. 2004. Specification Analysis of Option Pricing Models Based on Time-changed Lévy Processes. *Journal of Finance* 59: 1405–1440.
- Huang, J.-z., and M. Huang. 2003. “How Much of the Corporate-treasury Yield Spread Is Due to Credit Risk?” Working paper, Penn State University.
- Hull, J., I. Nelken, and A. White. 2004. Merton’s Model, Credit Risk and Volatility Skews. *Journal of Credit Risk* 1: 8–23.
- Hull, J., and A. White. 2000. Valuing Credit Default Swaps I: No Counterparty Default Risk. *Journal of Derivatives* 8: 29–40.
- Kalman, R. E. 1960. A New Approach to Linear Filtering and Prediction Problems. *Transactions of the ASME—Journal of Basic Engineering* D 82: 35–45.
- Kim, I. J., K. Ramaswamy, and S. Sundaresan. 1993. Does Default Risk in Coupons Affect the Valuation of Corporate Bonds?: A Contingent Claims Model. *Financial Management* 22: 117–131.
- Le, A. 2007. “Separating the Components of Default Risks: A Derivative-based Approach.” Working paper, New York University.
- Leland, H. E. 1994. Risky Debt, Bond Covenants and Optimal Capital Structure. *Journal of Finance* 49: 1213–1252.
- Leland, H. E. 1998. Agency Costs, Risk Management, and Capital Structure. *Journal of Finance* 53: 1213–1243.
- Leland, H. E., and K. B. Toft. 1996. Optimal Capital Structure, Endogenous Bankruptcy and the Term Structure of Credit Spreads. *Journal of Finance* 51: 987–1019.
- Li, H., M. T. Wells, and C. L. Yu. 2008. A Bayesian Analysis of Return Dynamics with Lévy Jumps. *Review of Financial Studies* 21: 2345–2378.
- Longstaff, F. A., S. Mithal, and E. Neis. 2005. Corporate Yield Spreads: Default Risk or Liquidity? New Evidence from the Credit-Default Swap Market. *Journal of Finance* 60: 2213–2253.
- Longstaff, F. A., and E. S. Schwartz. 1995. A Simple Approach to Valuing Risky Fixed and Floating Rate Debt. *Journal of Finance* 50: 789–819.
- Madan, D. B., P. P. Carr, and E. C. Chang. 1998. The Variance Gamma Process and Option Pricing. *European Finance Review* 2: 79–105.
- Mella-Barral, P., and W. Perraudin. 1997. Strategic Debt Service. *Journal of Finance* 52: 531–566.
- Merton, R. C. 1974. On the Pricing of Corporate Debt: The Risk Structure of Interest Rates. *Journal of Finance* 29: 449–470.
- Merton, R. C. 1976. Option Pricing When Underlying Stock Returns Are Discontinuous. *Journal of Financial Economics* 3: 125–144.



- Ronn, E. I., and A. K. Verma. 1986. Pricing Risk-adjusted Deposit Insurance: An Option Based Model. *Journal of Finance* 41: 871–895.
- Titman, S., and W. Torous. 1989. Valuing Commercial Mortgages: An Empirical Investigation of the Contingent Claim Approach to Pricing Risky Debt. *Journal of Finance* 44: 345–373.
- Todorov, V., and G. Tauchen. 2008. “Activity Signature Functions for High-frequency Data Analysis.” Working paper, Northwestern University and Duke University.
- Wan, E. A., and R. van der Merwe. 2001. “The Unscented Kalman Filter.” In S. Haykin (ed.), *Kalman Filtering and Neural Networks*. New York: Wiley.
- Zhou, C. 2001. The Term Structure of Credit Spreads with Jump Risk. *Journal of Banking and Finance* 25: 2015–2040.
- Zhu, H., Y. Zhang, and H. Zhou. 2005. “Equity Volatility of Individual Firms and Credit Spreads.” Working paper, Bank for International Settlements.